UNIVERSITEIT VAN PRETORIA
UNIVERSITY OF PRETORIA
YUNIBESITHI YA PRETORIA
Denkleiers • Leading Minds • Dikgopolo tša Dihlalefi

Comparative screening study on the adsorption of Aqueous Pb(II) using different Metabolically Inhibited Bacterial Cultures from industry

Patrick Yawo Kpai

Comparative screening study on the adsorption of Aqueous Pb(II) using Different Metabolically Inhibited Bacterial Cultures from industry

by

Patrick Yawo Kpai

A dissertation submitted in partial fulfillment of the requirements for the degree of

Master of Science (Environmental Technology)

in the

Department of Chemical Engineering

University of Pretoria

South Africa

June 2023

Abstract

The current study aimed at investigating the bioremediation removal effectiveness of Pb(II) by metabolically inhibited microbial cultures: a) Waste activated sewage sludge obtained from a local wastewater treatment plant (SS), commercially sourced industrial bioremediation microbes b) bran-based filler with bacteria (BB), and c) salt-and-starch based filler with bacteria (S&S), d) an industrially obtained Pb(II) remediating consortium (Cons), and purified strains of e) *Paraclostridium bifermentans* (PB), and f) *Klebsiella pneumoniae* (KP) isolated from the consortium. The study's focus was specifically targeted towards operational analysis. This study demonstrated that the metabolically inactive SS, BB, S&S, Cons, PB, and KP bacteria adsorbed 55.4 mg/g, 54.6 mg/g, 50.6 mg/g, 54.4 mg/g, 27.4 mg/g, and 23.1 mg/g of Pb(II) within 3 h, respectively. In addition, maximum adsorption capacities of 141.2 mg/g, 208.5 mg/g, 193.8 mg/g, 220.4 mg/g, 153.2 mg/g, and 217.7 mg/g were measured respectively. FTIR spectroscopy supported the chemisorption of Pb(II) onto functional groups as being responsible for this removal. Two-phase pseudo-first-order kinetics fits best described the adsorption kinetics of the adsorbents which might be as a result of the separation of fast and slow adsorption rates into separate compartments, thereby allowing for better representation of a heterogeneous surface. The Crank mass transfer model shows that external mass transfer is the main mechanism of Pb(II) removal due to the high molecular diffusivity of Pb(II) as compared to the effective diffusion coefficients of the metabolically inhibited adsorbents. The equilibrium isotherm was well described by two-surface Langmuir equilibrium isotherm model likely due to different adsorption sites with different adsorption energies which allows a comparably better description of the adsorption. The morphology of the adsorbents showed that the surface of the metabolically inhibited adsorbents was rough, coarse, with observable pores, and irregular

crevices. The results from the EDS analyses indicated the presence of Pb on the surface of the metabolically inhibited adsorbents confirming the adsorbents were able to remove Pb(II) from the aqueous systems. Recovery of Pb(II) from the biosorbents were further tested and showed 72.4 %, 68.6 %, 69.7 %, 69.6 %, 61.0 %, and 72.4 % for the SS, BB, S&S, Cons, PB, and KP bacteria, respectively.

The results demonstrate the remarkable potential of these low cost, self-generating biosorbents for the treatment of Pb(II) contaminated aqueous streams.

Keywords: adsorption, consortium, *K. pneumoniae*, *P. bifermentans,* lead, sewage sludge, bran-based filler bacteria, salt-and-starch filler bacteria.

Acknowledgements

My first appreciation goes to my Lord and Savior Jesus Christ for His guidance, protection, wisdom, grace, mercy, and strength throughout this journey.

Secondly, I would like to express my gratitude to the following people and organisations for their contribution to the research in this dissertation:

1. The financial assistance of Mastercard Foundation Scholarship, University of Pretoria.
2. National Research Foundation (NRF) for funding the research.
3. Prof H.G. Brink, my supervisor, and Prof E.M.N. Chirwa, my co-supervisor for their support and guidance.
4. Brandon van Veenhuyzen, Olga Neveling, Carla Cilliers, and Job Tendenedzai for my training.

Publications

1. Kpai P.Y., Chirwa E.M.N., Brink H.G., 2022, Biosorption of Aqueous Pb(II) by a Metabolically Inactive Industrial Klebsiella pneumoniae Strain. Chemical Engineering Transactions, 96, 373–378.
2. Kpai P.Y., Chirwa E.M.N., Brink H.G., 2022, Biosorption of Aqueous Pb(II) by a Metabolically Inactive Battery Recycling Plant Consortium: The Role of Paraclostridium bifermentans Microbial Strain. Chemical Engineering Transactions, *in press*.

Conference Presentations

1. 1st International Conference On Energy, Environment & Digital Transition (E2DT), Milano, Italy, 23-26 October, 2022: Oral Presentation: Biosorption of Aqueous Pb(Ii) by a Metabolically Inactive Industrial *Klebsiella pneumoniae* Strain
2. The 18th IWA Leading Edge Conference on Water and Wastewater Technologies Achieving Sustainability Through Water Technology (LET2023), Daegu, South Korea, 29 May – 2 June, 2023: Poster Presentation: Biosorption of aqueous Pb(II) by a metabolically inactive battery recycling plant consortium: The role of *Paraclostridium bifermentans*

Nomenclature

ATR – FTIR Attenuated total reflection-Fourier transform infrared

DMSO dimethyl sulfoxide

FTIR Fourier transform infrared

MTT 3-(4,5-dimethylthiazol-2-yl)-2,5-diphenyl tetrazolium bromide

OD_{600} Optical density at 600 nm

WWTP Wastewater treatment plant

SS Sewage sludge

BB Bran – based filler bacteria

S & S Salt – and – based filler bacteria

PB *Paraclostridium bifermentans*

KB *Klebsiella pneumoniae*

Table of Contents

List of Figures

List of Tables

1. Introduction

Lead is found throughout our environment, however, an increased amount in our environment comes from human activities including burning fossil fuels, mining, and manufacturing (Tiwari et al., 2013). This is very problematic because of the toxicity of lead and its tendency to bioaccumulate in ecosystems (Van Veenhuyzen et al., 2021b). Additionally, the presence of lead in wastewater is a major concern because of the health risks associated with lead consumption (Neveling et al., 2022). These health risks include but not limited to kidney damage, decreased IQ, memory scores capacity, learning ability, and other cognitive declines (Mason et al., 2014; Jakubowski, 2011; Klingberg, 2010). Also, due to the decrease in global lead reserves (Statista, 2019), lead recovery from wastewater streams is of ultimate importance as it offers an economic incentive (Van Veenhuyzen et al., 2021b).

Conventional techniques such as membrane filtration, adsorption, chemical precipitation, ion exchange, and electrodialysis are employed in addressing lead pollution from waste streams by converting Pb(II) ions to a less harmful state but require supplementary treatment in the recovery of Pb (0) (Van Veenhuyzen et al., 2021a). Additionally, many of these techniques suffer the problems of low efficiency and high operating costs (He et al., 2019). However, adsorption has certain merits over conventional methods such as high efficiency, minimising chemical and biological sludge, regeneration of adsorbents, low cost, and the possibility of metal recovery (Gupta et al., 2021).

Conventional and commercial adsorbents such as activated carbon (Abbaszadeh et al., 2016) are expensive to manufacture, difficult to expose, and involves cumbersome regeneration processes, whiles non-conventional adsorbents are cheap, has great complexing capacity, and is abundantly available (Hussain et al.,

2021). Selecting the most appropriate adsorbent is therefore a crucial step for an efficient adsorption process.

This research is a comparative screening study which investigated the bioremediation removal effectiveness of Pb(II) by metabolically inhibited microbial cultures: sewage sludge, two commercially sourced industrial bioremediation microbes (bran-based filler bacteria and salt-and-starch based filler bacteria), a Pb(II) resistant consortium and two microbial strains isolated from the consortium (*Klebsiella pneumoniae* and *Paraclostridium bifermentans*). This method of bio-removal is aimed towards scaling the process for large-scale implementation in various industries as a simple cost-effective method to remediate and regenerate Pb-containing effluents.

The main objectives of this research for this dissertation were:

1. Successfully grow commercially sourced industrial bioremediation microbes (bran-based filler bacteria and salt-and-starch based filler bacteria) in sewage.
2. Successfully inhibit the metabolic activity of the microorganisms in ensuring that a passive process was responsible for Pb(II) removal.
3. Measure, model, and compare the adsorption capacities of the metabolically inhibited adsorbents.
4. Characterise the surface properties of the metabolically inhibited adsorbents.
5. Determine the feasibility of Pb(II) desorption and subsequently reusability of the metabolically inhibited adsorbents.

These objectives were achieved through adsorption kinetics studies, adsorption equilibrium studies, and adsorbents surface analyses which are presented in the same order that they were executed.

2. Literature

2.1 Lead

Lead is a soft metal that occurs naturally in the form of lead sulphide (galena), and lead carbonate (cerussite) (Gupta et al., 2021). It is a bluish-grey-colored heavy metal with a low melting point (Debnath et al., 2019). Lead can be found in the Earth's crust, especially where geochemical weathering and volcanic activities occur. However, rapid industrialization and unplanned urbanization have introduced heavy metals into the environment through improper dumping of industrial wastes directly on land and into water bodies (Dixit et al., 2015). Through effluent discharges from various manufacturing processes, heavy metals, such as lead, copper, mercury, nickel, and chromium commonly enter aquatic systems resulting in damages to ecosystems and human health (Amarasinghe and Williams, 2007; Yarkandi, 2014). Mining, smelting, and processing of lead and lead-containing metal ores generate the greatest part of lead emissions from stationary sources (World Bank Group, 1998). Heavy metal contamination, especially lead, has been a constant common problem worldwide (Tong et al., 2000). Lead is the most common and one of the most toxic pollutant among all heavy metal pollutants, reaching water sources from various industrial activities such as metal plating and finishing, mining, oil refining, and battery manufacturing (Yarkandi, 2014; Mouflih et al., 2006). The worrying form of lead pollution is in an ionic or aqueous form, that is Pb(II) (Van Veenhuyzen et al., 2021a).

The allowable maximum concentration of lead in drinking water by the Environmental Protection Agency (EPA) and the World Health Organization (WHO) is 15 and 50 μg/L, respectively (Mahmud et al., 2016). The allowable limit of dissolved lead in wastewater in South Africa according to the Department of Water Affairs (2013) is 0.01 mg/L (10 μg/L). Serious health problems can

occur as a result of high lead concentrations (Mouflih et al., 2006). Lead poisoning can cause anemia, kidney damage, and toxicity symptoms including impaired kidney function, headache, and hypertension (Singh et al., 2008). According to Panchanadikar and Das (1994), the presence of lead in drinking water above the permissible limit causes diseases such as anemia, encephalopathy, hepatitis, and nephrotic syndrome. Chronic exposure to heavy metals such as lead poses a major threat to soil, water, and food safety because of their inherent toxicity to living organisms, especially humans (Fewtrell et al., 2004).

The world reserve of lead is estimated in 2019 at 90.4 million tonnes (USGS, 2019). Approximately 4.49 million metric tons of lead were extracted from mines worldwide in 2020 (Statista, 2021). Close to 5 million tonnes of lead ores are mined annually which are refined and used in a variety of industrial applications (ILA, 2019). Lead recovery is of ultimate importance as it does not only lead to an environmentally friendly cycle but also results in the diminution of the adverse effects of lead mining.

2.1.1 Lead contamination in South Africa

Industrial wastewater contamination is a striking problem in South Africa, a rapidly developing country where freshwater are scarce resources (Iloms et al., 2020), as the country is classified as water stressed (DWS, 2011). The second position with regards to sources of water in South Africa are effluents produced from industrial and domestic activities which currently is a major source of chemical and microbial pollution (Chetty and Pillay, 2019; Sibanda et al., 2015).

A study conducted by Iloms et al (2020) at Leeuwkuil, Gauteng Province, South Africa shows the need for improved technologies for lead removal from wastewater. The study was aimed at determining Pb(II) concentrations in

influents and effluents from the wastewater treatment plant (WWTP) and in different industrial wastewater as shown in Table 2.

The allowable limit of dissolved lead in wastewater in South Africa according to the Department of Water Affairs (2013) is 0.01 mg/L. The level of dissolved lead present in the effluent of the wastewater treatment plant and in all the industries exceeded the allowable limits.

Table 1: Concentrations of dissolved lead (mg/L) in the different industrial wastewater and Leeuwkuil WWTP influents and effleunts of the Vaal triangle, South Africa (Iloms et al., 2020)

Source of wastewater	Dissolved Pb (mg/L)
Industry 1: Battery	4.64 ± 0.17
Industry 2: Iron / metal galvanizing	0.18 ± 0.02
Industry 3: Iron / steel	0.18 ± 0.03
Industry 4: Tanking / car wash	0.19 ± 0.03
Industry 5: Iron / steel	0.21 ± 0.00
WWTP influent	0.20 ± 0.03
WWTP effluent	0.19 ± 0.03

A study conducted by Shamuyarira & Gumbo (2014) on the assessment of heavy metals in municipal sewage sludge in various municipalities in the Limpopo Province, South Africa shows that two municipalities (Polokwane and Louis Trichardt) have sewage sludge exceeding the allowable limit of 100 mg $(kg\ dry\ mass)^{-1}$ as shown in Table 2.

Table 2: Amount of dissolved lead in municipal sewage sludge in various municipalities of the Limpopo Province (Shamuyarira & Gumbo, 2014)

Municipality	Dissolved Pb (mg$(kg\ dry\ mass)^{-1}$)
Thohoyandou	34.56
Polokwane	102.8
Tzaneen	52.26
Louis Trichardt	171.90
Musina	21.28

Impact of lead on environmental health

Lead as an environmental contaminant can be found in the soil, air, water, and even our homes which poses a health hazard to the public. Being a metal, lead cannot be degraded, and this stability makes it a persistent toxic substance in the environment. The most common application of lead is in the manufacturing of lead acid batteries for energy storage which are mostly used in automotive applications as well as emergency power supplies for various critical services such as hospitals, communication networks, public buildings, and emergency services (Van Veenhuyzen, 2021a).

The United States Geological Survey estimates that only 17 years' supply of global raw workable lead reserves is available (Hörstmann et al., 2020). Lead recovery is of ultimate importance as it does not only lead to an environmentally friendly cycle but also results in the reduction of the negative impacts of lead mining.

An increased amount of lead in our environment comes from human activities including burning fossil fuels, mining, and manufacturing (Tiwari et al., 2013). Exposure of human populations to environmental lead was relatively low before the industrial revolution but has increased with industrialization and large-scale

mining (Tong et al., 2000). Industries such as mines and refineries introduce lead into the environment through smelting operations, combustion of fossil fuels, and tailings from mining. Wastewater streams and spillage from oil processing, and landfill leachate from the disposal of lead-containing products release lead into the environment (Van Hille et al., 2003).

Untreated discharge or effluent from industries such as battery manufacturing, coating, automotive, aeronautical, and steel, printing, pigments, fuels, photographic materials, and explosive manufacturing becomes a major source of lead contamination (Wong et al., 2003; King et al., 2007).

Heavy metals such as lead are non-biodegradable, bioaccumulate in tissues, and are biomagnified along with the trophic levels (Gray, 2002). Bioaccumulation and biomagnification increase the concentration of heavy metals such as lead in a biological organism or targeted organ over time until they become lethal to health (Mata et al., 2008). Lead is not essential as trace element to nutrition, nor does it serve any biological purpose in humans or animals, however, it can poison organisms including humans even in low concentrations as its bio-accumulates and biomagnifies in the food chain.

Heavy metal contamination such as lead is a growing concern due to its toxicity, bioaccumulation, long persistence, and increasing contamination in water and soil which poses a serious threat to the environment as well as human beings (Tao et al. 2012). Lead exposure in plants causes necrosis, and reduction in biomass and it inhibits growth (Bilal Shakoor et al., 2013).

Impact of lead on human health

Lead is one of a limited class of elements that can be described as purely toxic (Tiwari et al., 2013). Lead causes environmental and health problems because of its stability in the contaminated sites and the complexity of its mechanism in biological toxicity, particularly hazardous for children leading to mental

retardation when existing with an abnormal concentration in body fluid (Tiwari et al., 2013).

Signs and symptoms of lead poisoning in newborn (ages 0 – 4 weeks), infant child (ages 4 weeks – 1 year), toddler (ages 1 – 3 years), preschooler child (ages 4 – 6 years), adolescent (ages 12 – 19 years), adults (ages 20 – 39 years), and young adults (ages 40 – 64 years) are premature birth, lower weight, slowed growth, sluggishness, seizures, high blood pressure, and sperm count decreases (Debnath et al., 2019).

Lead affects cognitive parameters such as intelligence, memory, executive functioning, processing speed, language, and motor skills (Debnath et al., 2019). The effects of lead toxicity are decreased IQ, memory scores capacity, learning ability, and other cognitive declines (Mason et al., 2014; Jakubowski, 2011; Klingberg, 2010), decreases executive functioning abilities (Blair and Ursache, 2011), and impedes verbal concept formation (Richards and Rodgers, 2014). Lead poisoning causes brain damage and mental retardation in children (Moncrieff et al., 1964; Gibson et al., 1967). The health impacts of lead exposure in both children and adults are well documented, and no safe blood lead level in children has been found (Brown and Margolis, 2012).

In South Africa, it was reported that blood lead levels in children remained significantly high over the period studied hence the need for vigilant control of all sources of lead in the urban environment (Schirnding et al., 2001). In urban slums, lead poisoning is the main cause of brain damage, mental deficiency, and serious behavior problems among young children (Chisolm, 1971).

People with prolonged exposure to lead may be at risk for high blood pressure, heart disease, kidney disease, and reduced fertility (CDC, 2021). Lead targets tissues and organs including the heart, bones, intestines, kidneys, and the reproductive system, thus capable of disrupting metabolic processes and

threatening lives (Seiler et al., 1994; Deng et al., 2006). The Department of Health and Human Services (DHHS), Environmental Protection Agency (EPA), and the International Agency for Research on Cancer (IARC) have determined that lead is probably cancer-causing in humans.

Lead concentrations and exposure time are key factors when measuring lead toxicity. Acute toxicity occurs when an individual is exposed to high concentrations of lead within a short period of time which can result in coma, seizures, or death. However, when one is exposed to low concentrations of lead for a long period of time, it leads to chronic poisoning which can cause diseases such as anemia, neurotoxicity, hemotoxicity, nephrotoxicity, and reduced fertility (Tiwari et al., 2013).

Regulations have been implemented by regulatory organisations globally regarding the acceptable limits for the discharge of heavy metal in the aquatic environment with intervention through ISO 14000 aimed at controlling contamination. The US Centres for Disease Control and Prevention has defined an elevated blood lead level in children as <10 μg/dL, based on neurologic toxicity (Tiwari et al., 2013).

Due to the increasing concern about public health and environmental problems caused by lead contamination, developing highly efficient and stable treatment methods is necessary (Jeong et al., 2019).

Lead removal techniques from wastewater

Removal of pollutants such as lead from wastewater has conventionally been achieved through a range of chemical and physical processes (Kiran et al., 2007; Cesur and Baklaya, 2007). The conventional processes for removing heavy metals from wastewater include many processes such as chemical precipitation, flotation, adsorption, ion exchange, and electrochemical deposition, however,

chemical precipitation is the most widely used for heavy metal removal from inorganic effluent (Barakat, 2011).

To date, much effort has been dedicated to developing an efficient treatment method for removing Pb(II), such as ion exchange, solvent extraction, adsorption, membrane filtration, precipitation, and reverse osmosis (Merganpour et al., 2015). These processes have significant disadvantages, which are, for instance, incomplete removal, high-energy requirements, and the production of toxic sludge (Eccles, 1999).

The use of high-end treatment systems such as ion exchange, reverse osmosis, electrodialysis, and ultrafiltration involves a high cost to achieve desirable removal percentages or to meet the compliance level (Ahalya et al., 2003). Generally, the use of low-end treatment systems such as chemical precipitation is applied in the removal of heavy metal from industrial wastewater due to its simple operation and cost-effectiveness.

Most of these treatment techniques are advantageous due to high selectivity but are too costly in the treatment of waste streams with low Pb(II) concentrations (Fu and Wang, 2011). The traditional approaches for the removal of Pb(II) include reduction, extraction, ion exchange, precipitation, and membrane filtration which suffer the problems of low efficiency and high operating costs (He et al., 2019).

Various processes are available to remove Pb(II) from industrial effluent (Van Veenhuyzen, 2021). Table 3 present a summary of the process description of the most widely employed treatment technologies for heavy metal removal from wastewater.

Table 3: Conventional treatment technologies employed for heavy metal removal from wastewater.

Method and Description	**Advantages**	**Disadvantages**	**Reference(s)**
High-end technology			
Ion-exchange – Metal ions from dilute solutions are exchanged with ions held by electrostatic forces on the exchange resin.	Rapid operation, high selectivity, and treatment capacity.	Expensive and partial removal of certain ions.	Lee et al., 2006.
Reverse osmosis – Metal ions are separated using semi-permeable ion selective membranes. An electrical potential between the two electrodes cause a separation of cation and anion, thus cells of concentrated and dilute salts are formed.	High recovery of water.	Metal hydroxides formed clogged the membrane.	Sadrzadeh et al., 2008.
Ultrafiltration – Pressure driven membrane filtration	Very fast reaction kinetics, aqueous based	Expensive. Generation of sludge.	Aliane et al., 2001.

operations that use porous membranes for the removal of heavy metals.	processing, and high selectivity of separation.		Yurlova et al., 2002.
Low-end technology			
Chemical precipitation – Precipitation of metal ions achieved by the addition of coagulants such as iron salts, alum, and lime.	Low capital cost	Sludge generation	Dang et al., 2009. Matlock et al., 2001.

2.1 Bioremediation

Bioremediation is the process of using microorganisms such as bacteria, algae, fungi, and plants to break down, change, remove, immobilize, or detoxify various physical and chemical pollutants in the environment (Bala et al., 2022).

Bioremediation is a cost-effective and practical solution for removing environmental contaminants (Tripathi et al., 2021). Bioremediation methods also have advantages such as low-cost requirements, fewer environmental influences, and no secondary pollution (Ateia et al., 2016).

However, for microorganisms to combat contaminants, they must get into contact with compounds that supply them with the energy and nutrients they need to proliferate. There are several factors such as physical, chemical, biological, soil-type, carbon and nitrogen source, type of microorganisms, i.e., single or consortium, and others that affect the process of bioremediation (Garg et al., 2012). Microbial consortiums often have both multifunctionality and resistance

because different species work together to use all substrates in the best way possible, thereby increasing the bioremediation efficiency compared to single microorganism (Abatenh et al., 2017).

Environmental contamination by heavy metals has emerged as a major concern (Hashem et al., 2017) and is associated with environmental pollution and bio-toxicity issues attributed to their ability to inhibit biodegradation activities (Masindi and Muedi, 2018). Bioremediation is a technique for removing or converting harmful contaminants like heavy metals into less harmful substances by employing dead or alive biomass (Kapahi and Sachdeva, 2019).

Wastewater treatment using microorganisms is being exploited globally as it is economical, environmentally friendly, and sustainable (Saxena et al., 2020).

It has been revealed through much research that bioremediation can be an effective solution for water treatment because of the capability of microbes to survive, adapt, and thrive within different environments including wastewater (Palma et al., 2017; Sharma and Khan, 2013; Singh et al., 2016; Wuang et al., 2016). Bioremediation is an attractive technique due to the availability of biomaterials such as fungi, bacteria, algae, and plants and its potential for low cost and high efficiency at low concentrations of pollutants (Kang et al., 2015).

2.2.1 Factors affecting bioremediation

The factors that affect bioremediation procedures include but are not limited to; the presence of a microbial community efficient in degrading the contaminants, the accessibility of contaminants to the microbial population, and environmental factors such as temperature, pH, nutrients, and the presence or absence of oxygen (Saxena et al., 2020). Nutrients such as carbon, nitrogen, and phosphorous are required by microorganisms for survival and continuous microbial activities (Couto et al., 2014; Jamwal et al., 2013). pH in the range of 6.5 – 8.0 is the optimum condition for effective bioremediation as it plays a major role in the

solubility and the biological availability of nutrients and other constituents to the microbes (Saxena et al., 2020). The ideal temperature range for microbial growth is from 25 – 45 °C (ESTCP, 2005). To an extent, the biodegradation rate rises with increasing temperature and decreases with decreasing temperature (Saxena et al., 2020).

2.2.2 Advantages and disadvantages of bioremediation

The advantages and disadvantages of bioremediation are summarized in Table 4 below:

Table 4: Advantages and disadvantages of bioremediation. Reproduced from (Pacheco et al., 2015).

Advantages	Disadvantages
A safe natural process for the environment.	Process is limited to biodegradable compounds.
The process is cost-effective as it eliminates transportation and operation costs.	There are concerns about some degrading compounds being more toxic than the parent compound.
The process does not generate waste.	The process lasts much longer than other treatment methods such as excavation and incineration.
It may be combined with other treatment technologies.	Biological processes are often highly specific.
Can be made directly on-site with no disruption to ecosystem.	

2.3 Adsorption of aqueous Pb(II)

Adsorption describes a mass transfer mechanism whereby contaminants are transferred from the liquid phase onto a solid surface (Wang and Guo, 2020) as shown in Figure 1. Biosorption involves the physico-chemical adsorption mechanisms to materials of biological origin (Robalds et al., 2016). Adsorption which is a surface phenomenon in which a solution containing the adsorbate gets adsorbed on the surface of the adsorbent can be of two types, that is physisorption and chemisorption (Hussain et al., 2021).

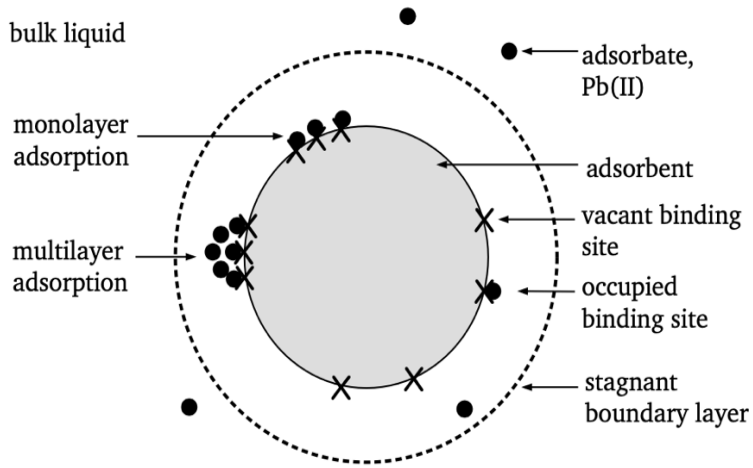

Figure 1: Visualisation of adsorption terminology. Adapted from Tran et al. (2017).

Physisorption involves the binding of the adsorbate to the adsorbent due to van der Waals forces whiles chemisorption involves the binding of the adsorbate due to chemical reactions. Physisorption is a weak, reversible and usually endothermic reaction while chemisorption is an irreversible, selective, and generally exothermic reaction (Tripathi and Ranjan, 2015; Singh and Gupta, 2016; Freundlich, 1906).

Ion exchange is the biosorptive uptake of heavy metals by microorganisms because of the exchange of the bivalent metal ions and the cell walls of the microorganisms (Perpetuo et al., 2011).

Bioprecipitation is the use of microorganisms, especially bacteria in producing metabolites which react with metals present in the wastewater and thereby forming metal precipitates, by converting metals from its aqueous phase into a solid phase (Janyasuthwiong and Rene, 2017).

Precipitation, ion-exchange, physiosorption, and chemisorption are the four main mechanisms identified for an efficient adsorption of pollutants (Davis et al., 2003; Veglio and Beolchini, 1997). The sorption mechanisms of classification as proposed by Robalds et al. (2016) is shown in Figure 2.

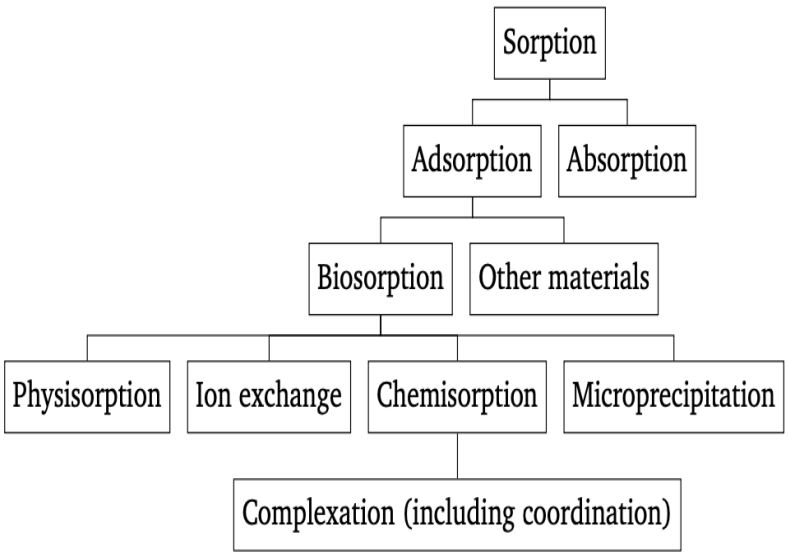

Figure 2: Classification of sorption mechanisms as proposed by Robalds et al. (2016). Adapted from van Veenhuyzen et al. (2021b).

The main advantage of adsorption as compared to other wastewater treatment technologies is the production of a high-quality effluent, efficient, and its cost-effectiveness (Hussain et al., 2021). Additionally, most adsorbents can be

regenerated and used further (Ojedokun and Bello, 2016), and it is an environmentally friendly technique (Demirbas, 2008).

Some of the important criteria in selecting adsorbents include their cost effectiveness (Hussain et al., 2021), distribution of functional groups, high surface area, and their polarity (Vunain et al., 2016; Ewecharoen et al., 2009). Examples of conventional and commercial adsorbents are activated carbon (Abbaszadeh et al., 2016), carbon nanotubes (Mubarak et al., 2014), zeolites (Huang et al., 2018), and graphenes (Carpio et al., 2014) and fullerenes (Nimibofa et al., 2018).

The activated carbons are expensive to manufacture, difficult to expose, and cumbersome regeneration process, whiles non-conventional adsorbents are cheap, great complexing capacity, and abundantly available (Hussain et al., 2021). Selecting the most appropriate adsorbent is a crucial step for an efficient adsorption process.

Adsorption has become one of the alternative treatments due to its low cost, high performance, and wide pH range, in recent years, the search for low-cost adsorbents that have metal-binding capacities has intensified (Leung et al., 2000). Adsorption has certain merits over conventional methods such as high efficiency, minimising chemical and biological sludge, regeneration of adsorbents, low cost, and the possibility of metal recovery (Gupta et al., 2021). The adsorbents may be of mineral, organic or biological origin, zeolites, industrial by-products, agricultural wastes, biomass, and polymeric materials (Kurniawan et al., 2005).

The performance of several adsorbents which were employed for Pb(II) removal as a measure of the percentage of Pb(II) removal are presented in Table 5.

Table 5: Biosorbents studied for Pb(II) bioremediation and their performance. Reproduced from (Van Veenhuyzen et al., 2020).

Microorganism	Pb(II) (ppm)	Time	Pb(II) removal (%)	References
Bacillus sp.	450	11 h	90	Kafilzadeh et al., 2012
R. palustris	100	4 days	96	Sinha and Biswas, 2014
E. cloacae	7	48 h	68	Kang et al., 2015
Enterobacter sp.	1000	24 h	90	Jiang et al., 2019
Pseudomonas sp.			88	
Corynebacterium sp.			87	
Staphylococcus sp.			65	
Escherichia coli			60	

3. Materials and methods

3.1 Microbial culture

The SS bacteria was obtained from the active sludge pond at the Daspoort Wastewater Treatment Plant in Pretoria, South Africa (Coordinates: 25.7346° S, 28.1769° E), the commercially sourced industrial bioremediation microbes (BB and S&S bacteria) were obtained from Bemical CC, Johannesburg, South Africa. These (SS, BB, S&S) bacteria were cultivated by dosing 0.5 mL of the microbes into 100 mL of clarified sewage collected from the Daspoort Wastewater Treatment Plant.

The Pb(II)-resistant microbial consortium was obtained from lead-contaminated soil at a battery recycling plant in South Africa. This consortium has been demonstrated to remove 90 % of Pb(II) from an 80 mg/L solution over a period of 7 days (Brink et al., 2017). The consortium was effective at precipitating Pb(II) from the solution and was shown to remove approximately 50 % of Pb(II) at conditions of 80 ppm and 500 ppm within the first 3 hours (Hörstmann et al., 2020).

Klebsiella pneumoniae and *Paraclostridium bifermentans* were identified as the microbial strains present in the microbial consortium after using 16S rDNA sequencing and are likely the main organisms responsible for bioprecipitation of lead by Brink, Hörstmann & Peens (2020). FTIR spectroscopy supported the chemisorption of lead being responsible for the initial phase of Pb(II) removal which acts as a vehicle for concentrating Pb(II) on the surface of the bacteria before bioprecipitation takes place (van Veenhuyzen et al., 2021a).

The consortium inoculum was prepared by adding 1 g of Pb(II)-contaminated soil to a mixture of LB broth and 80 ppm Pb(II) in an anaerobic 100 mL serum bottle and incubated for 24 h at 35 °C at 120 rpm. Glycerol was added to the matured

inoculum to a final ratio of 20% v/v and stored cryogenically at −77 °C. The precultures were thereafter prepared from the cryogenically stored inoculum.

The microbial pure cultures preparation (*P. bifermentans* and *K. pneumoniae*) is described by Neveling et al. (2022) on the study of Microbial Precipitation of Pb(II) with Wild Strains of *Paraclostridium bifermentans* and *Klebsiella pneumoniae* Isolated from an Industrially Obtained Microbial Consortium.

The 100 mL Cons, PB, and KP cultures were prepared under aerobic conditions in a batch reactor starting with 20 g/L tryptone, 10 g/L yeast extract, and 1 g/L NaCl (Hörstmann et al., 2020). The cultures were left to grow in a shaker incubator for 24 h at 35 °C and 120 rpm.

All cultures (SS, BB, S&S, Cons, PB, and KP) were centrifuged at 9000 rpm for 10 minutes at 4 °C, rinsed with ultrapure water, and centrifuged again before being oven dried at 74 °C for 24 h (Tan et al., 2017; Sastri, 2022) to successfully inhibit metabolic activity and ensure Pb(II) removal through adsorption alone.

3.2 Preparation of lead nitrate solution

The $Pb(NO_3)_2$ solution was prepared using 1.6 g of lead nitrate (Glassworld, South Africa) added to 100 mL ultrapure water. This produces a Pb(II) solution of 10 000 mg/L.

3.3 Metabolic activity measurement

Metabolic activity measurements were conducted with the aid of 3-(4,5-dimethylthiazol-2-yl)-2,5-diphenyl tetrazolium bromide (MTT) which is a yellow dye reduced to formazan crystals and the organic solvent dimethyl sulfoxide (DMSO) at a wavelength of 550 nm (Sigma Aldrich, St. Louis, MO, USA) (Hörstmann et al., 2020). For metabolic activity readings, 0.5 mL filtered (0.45 µm) of the sample was added to 0.2 mL MTT and 1.3 mL sterilized ultrapure water. Also, 0.5 mL unfiltered sample was added to 0.2 mL MTT and 1.3 mL

sterilized ultrapure water. Dimethyl sulfoxide was added to the solution after an hour of incubation to dissolve the formazan crystals (Van Veenhuyzen et al., 2021a). A spectrophotometer was used in measuring light absorbed at 550 nm between the unfiltered and filtered samples to infer metabolic activity differences (Peens, 2018).

3.4 Optical density measurement

A spectrophotometer was used in reading the degree of light dispersed by the pure culture. For optical density reading (OD_{600}), the sample was diluted 4 times before measurement was made at 600 nm.

3.5 Dry mass measurement

The dry mass of bacteria per mL of culture was determined by centrifuging a portion of the culture at 9000 rpm for 10 min at 4 °C, rinsing with distilled water, and centrifuging again (Van Veenhuyzen et al., 2021a) before being oven dried at 74 °C for 24 h before weighing.

3.6 Lead removal experiments

Sterilized reactors containing 100 mL of ultrapure water, 1 ml of 1.711 M $NaNO_3$ salt substitute with metabolically inhibited bacteria, and 100 ppm of Pb(II) were prepared. This will serve as the concentration for the basis of comparison with other microbial strains of the consortium. The reactor was triplicated to ensure repeatability and the Pb(II) removal over a 14 h period was investigated.

Reactors were sampled at various time intervals and filtered (0.45 µm) and initial and final pH readings of the samples were measured. The Pb(II) concentration in samples was measured using atomic absorption spectroscopy (Perkin Elmer AAnalyst 400, Waltham, Massachusetts).

The adsorption capacity of the adsorbents was computed according to equation (1):

$$q_t = \frac{(C_o - C_f)V}{W} \qquad (1)$$

Where q_t is the adsorption capacity (mg/g), and C_o and C_f are the initial and final concentrations (mg/L) respectively, V is the volume of the solution (L), and W is the dry mass of adsorbent (g).

3.7 Adsorption kinetics

The measure of adsorption uptake at a constant concentration with respect to time is adsorption kinetics (Tawfik, 2022). Pseudo-first-order kinetic model was derived from the Freundlich isotherm by Ezzati (2019). This model can describe the diffusional adsorption (Guo and Wang, 2019). Pseudo-second order kinetic model assumes that the rate of adsorption of solute is proportional to the available sites on the adsorbent, and the reaction rate is dependent on the amount of solute on the surface of the adsorbent, the driving force $(q_e - q_t)$ is proportional to the number of active sites available on the adsorbent (Kajjumba et al., 2018).

The sampled adsorptions were fit to a pseudo-first order, two-phase pseudo-first order, and a pseudo-second order isotherms as described in Equation 2 (Tan and Hameed, 2017), Equation 3 (Wang et al., 2011), and Equation 4 (Tan and Hameed, 2017) respectively.

$$Q(t) = Q_e[1 - \exp(-k_1 t)] \qquad (2)$$

$$Q(t) = Q_{e,fast}\left[1 - \exp(-k_{1,fast} t)\right] + Q_{e,slow}\left[1 - \exp(-k_{1,slow} t)\right] \qquad (3)$$

$$Q(t) = \frac{Q_e^2 k_2 t}{1 + Q_e k_2 t} \qquad (4)$$

where Q_e is the value of Pb(II) adsorbed at equilibrium in mg/g, t is time in min, k_1 and k_2 are the rate constants in 1/min and g/(mg min) for pseudo-first and

pseudo-second order respectively. The sum of $Q_{e,fast}$ and $Q_{e,slow}$ in equation (3) gives the overall equilibrium adsorption capacity.

3.8 Diffusion Model of Crank

Crank's diffusion model (Crank, 1975) is based in the second law of Fick. It considers the diffusion of a compound in a specific directional coordinate, z, with time, t as shown in equation 5.

$$\frac{\delta m(t)}{\delta t} = \frac{\delta}{\delta z}\left(D_{ef}\frac{\delta m(t)}{\delta z}\right) \qquad (5)$$

where m(t) is the amount of the compound and D_{ef} is the effective diffusion coefficient.

Largitte and Pasquier (2016) described the internal mass transfer in equation 6.

$$\frac{\delta Q}{\delta t} = \frac{D_e}{r^2}\frac{\delta}{\delta r}\left(\frac{r^2\delta Q}{\delta r}\right) \qquad (6)$$

where D_e is the effective adsorbate diffusivity in m^2/s.

Effective adsorbate diffusivity, D_e can be calculated from equation (6) using the integrated solutions given by Boyd et al. (1947) as shown in equation (7).

$$\frac{Q}{Q_e} = 1 - \frac{6}{\pi^2}\sum_{n=1}^{\infty}\frac{1}{n^2}\,exp\left(-\frac{D_e\pi^2n^2t}{r^2}\right) \qquad (7)$$

Where q_t is the amount of Pb(II) adsorbed (mg/g) at a given time t (min) and k_p (mg/$g\ min^{1/2}$) is the intraparticle diffusion rate constant which was obtained from plotting q_t against $t^{0.5}$.

3.9 Adsorption equilibrium experiment

Batch adsorption experiments were carried out to predict the equilibrium behaviour of the adsorbents. Serum bottles containing 1.352 g/L of adsorbate were prepared with 100 mL of Pb(II) solution in concentrations ranging from 0

to 600 mg/L Pb and sealed with rubber stoppers. The serum bottles were agitated using a water bath shaker (Labotec EcoBatch Model 207) at a constant agitation speed of 120 rpm and maintained at temperatures of 25°C, 35°C, and 45°C. The pH, as well as lead concentrations, were measured well after equilibrium was reached (24 hrs) using atomic absorbance spectrophotometry (Perkin Elmer, Waltham, Massachusetts).

3.10 Adsorption isotherm

Adsorption isotherm model is a curve describing the phenomenon that governs the release of a substance from an aqueous media to a solid phase under constant conditions of temperature and pH (Boparai et al., 2011; Foo and Hameed, 2010; Kebede et al., 2016). This model is helpful in ascertaining the theoretical optimal adsorption power as well as the potential interactions between adsorbents and adsorbate (Bharathi and Ramesh, 2013). Langmuir, two-surface Langmuir, and Freundlich, models was used in evaluating the relationship between the adsorbate concentration and the amount adsorbed in the aqueous phase at equilibrium.

3.10.1 Langmuir isotherm

Adsorption isotherms help in describing the relationship between the adsorbate concentration and its respective equilibrium concentration at a constant temperature (Gawande et al., 2017). The Langmuir isotherm model is based on the equilibrium between adsorption and desorption kinetics and was proposed originally by Langmuir (1918). This model considers that the adsorption energy is constant over all sites on the surface and does not depend on the surface coverage, meaning the adsorption surface is homogenous and that the adsorbate is adsorbed at definite, localized sites and each site can accommodate only one adsorbent species, which implies that the adsorption on the surface is localised (Yang 1997; Do 1998).

The Langmuir isotherm equation as presented in equation (9) has two parameters that must be estimated from experimental data. That is the maximum adsorption capacity of the monolayer, q_{max}, and the Langmuir constant, K_L.

$$q_e = \frac{q_{max} K_L C_e}{1 + K_L C_e} \qquad (9)$$

Where q_e is the amount of Pb(II) adsorbed, q_{max} is the maximum amount of Pb(II) adsorbed (mg/g), C_e is the equilibrium concentration (mg/L), and K_L is the Langmuir constant (L/mg). q_{max} and K_L are related to adsorption capacity and energy of adsorption respectively (Zeng et al., 2004).

The maximum adsorption capacity, q_{max}, has a close relationship with the affinity of the adsorbent sites with the adsorbate, and the superficial area of the adsorbent and its value can be a function of the pH of the system as it modifies the affinity between the adsorbate and the adsorbent but not dependent on temperature (Do, 1998). The Langmuir constant, K_L, which is the equilibrium parameter is temperature dependent as it takes into account the kinetic equilibrium between adsorption and desorption (Do, 1998). The temperature dependence of the equilibrium parameter, K_L, is described by the van't Hoff's equation as presented in equation (10):

$$K_L = esp\left(\frac{\Delta S}{R} - \frac{\Delta H}{RT}\right) \qquad (10)$$

Where ΔH is the adsorption enthalpy and ΔS is the adsorption entropy.

A separation factor (R_L) which is a dimensionless constant defined by Webber and Chakkravorti (1974) is presented in equation (11):

$$R_L = \frac{1}{1 + K_L C_o} \qquad (11)$$

where K_L (L/mg) and C_o (mg/L) refers to the Langmuir constant and the adsorbate initial concentration respectively. The R_L value suggests the nature of the adsorption to be favorable ($0 < R_L < 1$), unfavorable ($R_L > 1$), or irreversible ($R_L = 0$) (Foo and Hameed 2010).

3.10.2 Two – surface Langmuir isotherm

The two-surface Langmuir isotherm model assumes that sorption takes place on two types of surfaces, each with different binding energies (Langmuir, 1918; Bolster and Hornberger, 2007). This model was presented by Irving Langmuir in his seminal paper on adsorption modelling (Langmuir, 1918). This model provides a mechanistic description of adsorption on heterogeneous surfaces (van Veenhuyzen et al., 2021b). The two-surface Langmuir isotherm model is presented in Equation (12):

$$Q_e = \frac{Q_{max,1} K_{L1} C_e}{1 + K_{L1} C_e} + \frac{Q_{max,2} K_{L2} C_e}{1 + K_{L2} C_e} \qquad (12)$$

3.10.3 Freundlich isotherm

The Freundlich isotherm model is used to represent nonlinear adsorption phenomenon (Freundlich, 1906) an used in describing non-ideal sorption on heterogeneous surfaces and multilayer sorption (Berkessa et al., 2019). It explains the physical sorption of the solute particle from metal solution to the adsorbent (Gupta et al., 2021). The model describes non-ideal, reversible, multilayer adsorption commonly employed for heterogeneous adsorbents such as biomass (Foo and Hameed, 2010). The Freundlich adsorption isotherm is summarised according to equation (13):

$$Q_e = K_F C_e^a = K_F C_e^{\frac{1}{n}} \qquad (13)$$

where Q_e is the amount of Pb(II) adsorbed at equilibrium (mg/g), C_e is the equilibrium concentration (mg/L), K_f is the Freundlich constant (L/mg), and n is the heterogeneity factor. The isotherm is linear when $a = 1$, favorable when $a < 1$, and unfavorable when $a > 1$ (Tran et al., 2017). Also, studies shows that a value for a between 0 and 1 shows surface heterogeneity, and values closer to 0 indicating more heterogeneous surfaces (Foo and Hameed, 2010). Adsorption data that suitably fits Freundlich adsorption isotherm shows that the solute sorbed on the exterior of the sorbent is forming many layers (Gupta et al., 2021).

3.11 Goodnesss of fit

Goodness of fit is used in determining which model best describe the interaction between the adsorbent and solute. The coefficient of correlation (R^2), sum-of-squared errors (SSE), standard error of estimates (Sy.x), and root mean squared error (RMSE) are some of the error functions employed to study model fit. Table 5 summaries the error function (Tan and Hameed, 2017; Subramanyam and Das, 2014; Demirbas et al., 2008, Kamal, 2020; Kajjumba et al., 2018).

Table 6: Common error functions

Error Function	Expression
Coefficient of correlation (R^2)	$\frac{\sum_{i=1}^{n}\left\|q_{cal} - \bar{q}_{exp}\right\|^2}{\sum_{i=1}^{n}\left\|q_{cal} - \bar{q}_{exp}\right\|^2 + \sum_{i=1}^{n}\left\|q_{cal} - q_{exp}\right\|^2}$
Sum-of-squared errors (SSE)	$\sum_{i=1}^{n}\left\|q_{cal} - q_{exp}\right\|_i^2$
Standard error of estimates (Sy.x)	$\sqrt{\frac{\sum_{i=1}^{n}\left(q_{cal} - \ddot{q}_{exp}\right)^2}{d_f}}$

Root mean squared error (RMSE)	$\sqrt{\frac{\sum(q_{cal} - q_{exp})^2}{n-2}}$

NB: q_{cal} is the calculated amount of adsorbate adsorbed, q_{exp} is the experimental amount of adsorbate adsorbed onto adsorbent, n is data points.

3.12 FTIR analysis

Fourier-transform infrared (FTIR) spectra of the cultures were measured after four successive processes. The first measurement was taken after 24 h growth period of the bacteria. The second measurement was taken after 24 h oven drying of the bacteria at 74 °C. The third measurement was taken after the bacteria was exposed to 100 ppm of $Pb(NO_3)_2$. The last measurement was taken 14 h after the addition of 100 ppm $Pb(NO_3)_2$ to the cultures. An attenuated total reflection (ATR) attachment was used in recording spectra on a Perkin Elmer Spectrum 100 FTIR spectrometer. All FTIR spectra were recorded on a wavelength from 4000 to 500 cm^{-1} and represent an average of 30 scans.

3.13 SEM - EDS Analysis

An ultrahigh-resolution filed emission scanning electron microscope (HR FESEM Zeiss Ultra Plus 55, Carl Zeiss AG, Oberkochen, Germany) with an InLens detector was used in studying the particle morphologies of the adsorbents. The scanning electron microscope was also fitted with an energy dispersive X-ray spectrophotometer (EDS) which was used in analysing the elemental composition of the metabolically inhibited adsorbents.

3.14 Regeneration

Regeneration experiments for the metabolically inhibited adsorbents were carried out using HNO_3 (Dai et al., 2016; Goyal et al., 2008; Van Veenhuyzen et al.,

2021b). For the regeneration, 1.48 g/L of the adsorbents were exposed to 200 mg/L initial Pb(II) for 24 h. Adsorbents were recovered afterwards with a filter paper and rinsed with distilled water before being dosed as 1.48 g/L into 0.1 M HNO_3 solution for 24 h (Van Veenhuyzen et al., 2021b). Atomic absorbance spectrophotometry (AA) was used in measuring the concentrations of Pb(II) for each step. Desorption efficiency was calculated using the equation below (Katsou et al., 2011):

$$\text{Desorption efficiency (\%)} = \frac{C_{de}}{C_{ad}}\ x\ 100 \qquad (18)$$

where C_{de} denotes the concentration of Pb(II) desorbed and C_{ad} is the amount of Pb(II) adsorbed. The recovered adsorbent was dried at 105 °C to constant mass (Bayuo et al., 2020), and so the regenerated adsorbent was used in adsorption – desorption cycles to determine the reusability of the metabolically inhibited adsorbents.

The amount of Pb(II) desorbed by each metabolically inhibited adsorbent into the solution per unit mass of adsorbent at equilibrium is calculated by (Katsou et al., 2011):

$$Q_d = \frac{C_{de}}{m}\ x\ V \qquad (19)$$

where Q_d is amount of Pb(II) desorbed in mg/g, C_{de} is the liquid phase Pb(II) concentration in the desorbing solution at equilibrium in mg/L, m is the mass of the adsorbents in mg, and V is the volume of the desorbing solution in mL.

4. Results and discussion

4.1 Lead removal experiments

It is found that the rate of adsorption of Pb(II) increased with an increase in contact time until the equilibrium is reached. Equilibrium was reached in 30 mins, 15 mins, 15 mins, 120 mins, and 60 mins in the bran – based filler bacteria (BB), salt – and – starch based filler bacteria (S&S), consortium (Cons), *P. bifermentans* (PB), and *K. pneumoniae* (KP), respectively. Equilibrium was not observed in the sewage sludge (SS) during 180 mins of investigation. Metabolically inactive Cons, PB, KP, SS , BB, and S&S removed 54.44 mg/g, 27.39 mg/g, 23.10 mg/g, 55.35 mg/g, 54.60 mg/g, and 50.63 mg/g of Pb(II) in 3 h respectively as shown in Figure 3. A passive process was responsible for Pb(II) removal from the solution as metabolic activity was not detected using MTT. Black or grey precipitate was not evident in the 14 h period, which indicates that neither PbS nor Pb (0) was formed.

Table 7: Variations in pH for adsorbents

Adsorbents	Initial pH	Final pH	Control
Cons	4.64	4.92	4.70
PB	4.63	4.74	4.66
KP	6.13	5.83	5.14
SS	5.08	5.70	4.82
BB	5.13	6.04	4.82
S&S	5.86	6.25	4.82

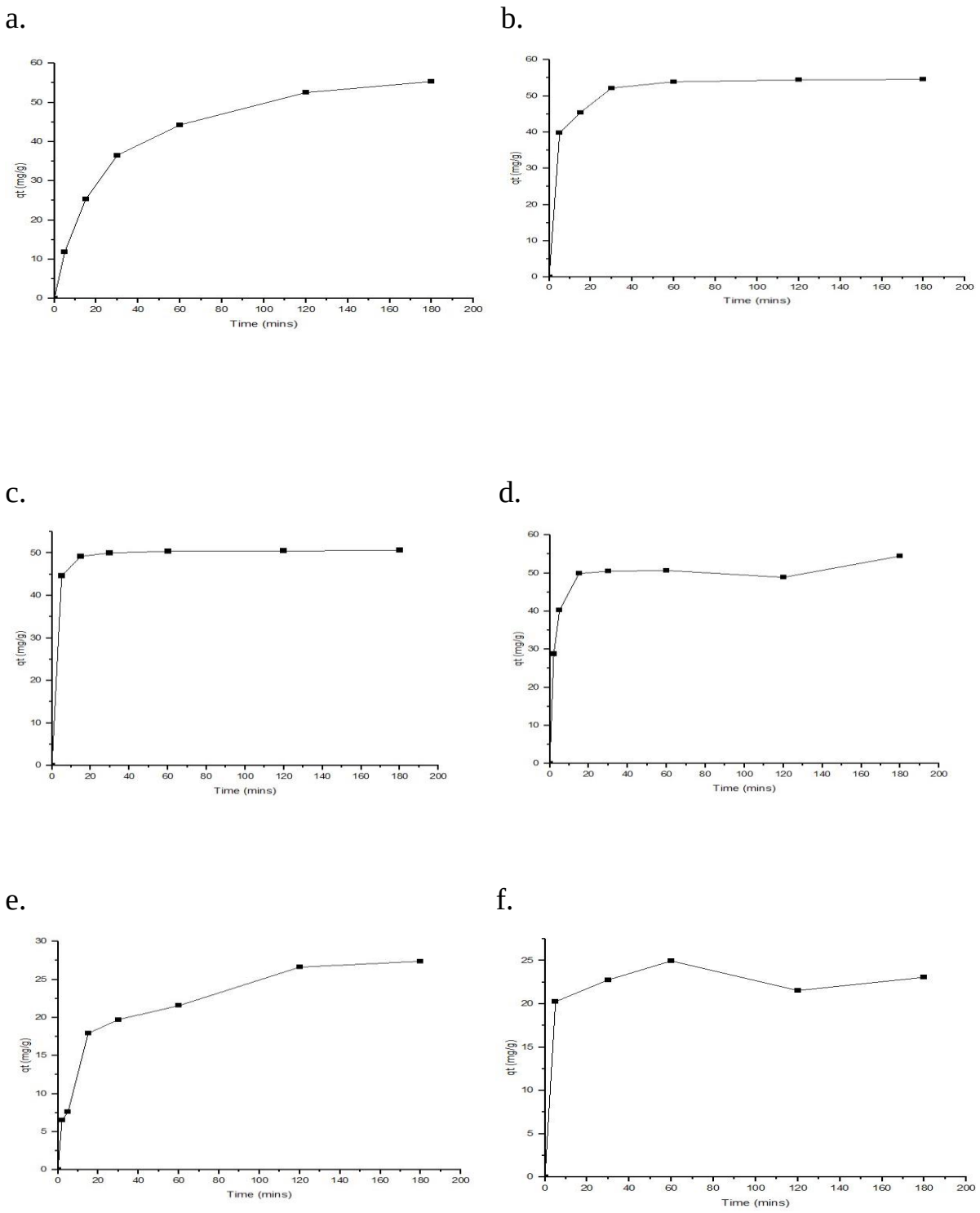

Figure 3: : Graph of Pb(II) adsorption by metabolically inhibited (a) SS, (b) BB, (c) S&S, (d) Cons, (e) PB, and (f) KP bacteria.

There was an increase in pH in the Cons, PB, SS, BB, and S&S. According to Gupta et al. 2021, higher pH promotes electrostatic attraction between negatively charged biosorbent surfaces and positively charged metal ions increasing

adsorption efficiency. The decrease in pH as observed in KP is likely due to the release of protons from the surface of the bacteria because of cation exchange processes in which the H^+ions are displaced by the Pb(II) ions on the surface (Van Veenhuyzen et al., 2021b).

4.2 Adsorption kinetics

Two-phase pseudo-first-order, pseudo-second-order, and pseudo-first-order kinetics were found to predict the behavior of the sorption processes for the SS, BB, S&S, Con, PB, and KP as shown in Appendix A in Figures 7, 8, and 9, respectively. The shaded areas represents 95% prediction interval which is the region where there is a 95% probability of future observation (Hyndman and Athanasopoulos, 2018). The parameters fit for two-phase pseudo-first-order, pseudo-second-order, and pseudo-first-order kinetic models are reported in Table 8, Table 9, and Table 10, respectively.

In all the experimental runs for all six adsorbents, it was found that two-phase pseudo-first-order kinetics fits had the highest coefficients of determination (average R^2 = 0.9939) and the lowest average sum of squares (SSE), standard error of estimates (Sy.x), and root mean square error (RMSE) of 5.91, 1.05, and 0.80 respectively. This might be as a result of the separation of fast and slow adsorption rates into separate compartments, thereby allowing for better representation of a heterogeneous surface (Van Veenhuyzen et al., 2021b).

It was also found that pseudo-second-order kinetic model (average $R^2 = 0.9914$) and an average sum of squares (SSE), standard error of estimates (Sy.x), and root mean square error (RMSE) of 9.30, 1.18, and 1.08, respectively represents the data better as compared to pseudo-first-order kinetic model (average $R^2 = 0.9818$) and with an average sum of squared errors (SSE), standard error of estimates (Sy.x), and root mean square errors (RMSE) of 24.87, 1.98, and 1.81 respectively. The better representation of pseudo-second-order kinetic model as

compared to pseudo-first-order kinetic model indicates an abundance of adsorption sites relative to Pb(II) ions in the solution (Wang and Guo, 2020; Guo and Wang, 2019). According to Vishan et al. (2019), this implies that valence forces may be involved in the sharing and exchange of electrons between the functional groups of the adsorbent and the adsorbate.

Based on the highest value of coefficient of determination (R^2) and the lowest sum of squared errors (SSE), standard error of estimates (Sy.x), and root mean square errors (RMSE), the adsorption kinetic model could be placed in the following sequence based on best – fitting model: Two-phase pseudo-first-order kinetic model > pseudo-second-order kinetic model > pseudo-first-order model.

From the best fitting model (two-phase pseudo-first-order kinetic model), the adsorption rates (k_{fast}) of the metabolically inhibited adsorbents could be placed in the following sequence for the fast phase: SS < PB < S&S < KB < Con < BB. However, based on the k_{slow} adsorption rate constant for the slow phase, the metabolically inhibited adsorbents could be placed in the following sequence: PB < SS < S&S < BB < KB < Con.

The result from the two-phase pseudo-first-order kinetic model shows that, BB has the fastest adsorption of Pb(II) (k_{fast}) whiles SS has the slowest adsorption of Pb(II). Results from the k_{slow} phase shows that the metabolically inhibited Cons has the fastest adsorption of Pb(II) in the slow phase as presented in Table 8. This might be due to longer periods of time required for BB to reach equilibrium, resulting in the smaller k_{slow} in the slow phase. This explains the high adsorption capacity of BB as compared to Con in the fast phase fraction and the low adsorption capacity of BB as compared to Con in the slow phase fraction.

In the pseudo-second-order kinetic model, which was the second-best fitting model, metabolically inhibited KP has the fastest rate constant (K_2) whiles SS has the slowest rate constant. Based on the rate constant (K_2), the metabolically

inhibited adsorbents could be placed in the following sequence: SS < PB < BB < Cons < S&S < KP. This implies that, using the pseudo-second-order model, the metabolically inhibited KP adsorbed Pb(II) faster than the rest of the metabolically inhibited adsorbents.

However, an evaluation of the error parameters and the value of $q_{e,cal}$ compared to the experimental value $q_{e,exp}$ shows that the metabolically inhibited KP adsorbent uptake of Pb(II) is better described by the pseudo-first-order kinetic model. This suggests that the rate limiting step of Pb(II) sorption onto the metabolically inhibited KP is dependent on the concentration of the Pb(II) in the adsorbate (Asuquo et al., 2016).

Table 8: Experimental data for two-phase pseudo-first order kinetics for metabolically inactive adsorbents.

Adsorbents	SS	BB	S&S	Cons	PB	KP
Best-fit values						
Q_t (mg/g)	58.04	54.62	50.55	51.16	31.15	23.14
PercentFast	48.71	62.60	94.02	40.31	54.99	84.33
$Q_{e,fast}$(mg/g)	28.27	34.19	47.53	20.62	17.13	19.51
$Q_{e,slow}$(mg/g)	29.77	20.43	3.02	30.54	14.02	3.63
k_{fast} (1/min)	0.08431	2.491	0.5131	1.113	0.1485	0.6623
k_{slow} (1/min)	0.01362	0.0601	0.05683	0.208	0.007895	0.1018
Ratio of rate constant	6.192	41.45	9.029	5.354	18.81	6.504
Goodness of Fit						
R^2	0.9997	0.9992	1	0.9929	0.9854	0.9863
SSE	0.7998	1.835	0.01289	16.53	10.33	5.946
Sy.x	0.5163	0.6772	0.06555	2.033	1.607	1.408
RMSE	0.3651	0.5529	0.04635	1.537	1.215	1.09

Table 9: Experimental data for pseudo-second order kinetics for metabolically inhibited adsorbents.

Adsorbents	SS	BB	S&S	Cons	PB	KP
Best-fit values						
Q_t (mg/g)	61.58	55.13	51.01	52.82	27.94	23.33
K_2(g/mg min)	0.0007604	0.008506	0.02839	0.01198	0.003404	0.05887
Goodness of Fit						
R^2	0.9993	0.9955	0.9998	0.9912	0.977	0.9853
SSE	1.781	10.47	0.3723	20.52	16.25	6.408
Sy.x	0.5968	1.447	0.2729	1.849	1.646	1.266
RMSE	0.5448	1.321	0.2491	1.712	1.524	1.132

Table 10: Experimental data of pseudo-first order kinetics of the metabolically inhibited adsorbents.

Adsorbents	SS	BB	S&S	Cons	PB	KP
Best-fit values						
Q_t (mg/g)	52.96	52.53	50.17	50.71	24.92	23.10
k_1(1/min)	0.0396	0.2635	0.439	0.3729	0.0749	0.4195
Goodness of Fit						
R^2	0.9891	0.9791	0.9995	0.9876	0.9494	0.9862
SSE	28.51	48.88	1.147	28.88	35.79	6.002
Sy.x	2.388	3.127	0.479	2.194	2.442	1.225
RMSE	2.18	2.854	0.4373	2.031	2.261	1.096

Results from the Crank mass transfer model (Appendix A: Figure 10 and Table 11) shows that the values of the effective diffusion coefficients (D_e) were in the same order of magnitude except for the metabolically inhibited SS and PB. The effective diffusion coefficients (D_e) for the metabolically inhibited SS, BB, S&S, Cons, PB, and KP are $2.57x10^{-13}\ m^2/s$, $2.40x10^{-12}\ m^2/s$, $5.69x10^{-12}\ m^2/s$, $3.50x10^{-12}\ m^2/s$, $4.54x10^{-13} m^2/s$, and $5.40x10^{-12}\ m^2/s$ respectively.

The order of the values of diffusion coefficients for the adsorbents are: S&S > KP > PB > Cons > SS > BB.

The low effective diffusion coefficients of the adsorbents as compared to the molecular diffusivity of Pb(II) which is 9.39 $x10^{-9}$ m/s (Sato et al., 1996) will result in the formation of thermodynamically stable structures due to the large time that Pb(II) must roam the surface of the adsorbents and attain the minimum energy configuration before attaching to the growing island nuclei (Otero, 2018). This suggests that external mass transfer (EMT) is the main mechanism of Pb(II) removal due to the high molecular diffusivity of Pb(II) as compared to the diffusion coefficients of the metabolically inhibited adsorbents. This agrees with literature as an adsorbate with a higher molecular diffusivity diffuse more rapidly through the bulk solution which results in the limited rate of mass transfer due to the slow diffusion within the boundary layer of the adsorbent with a lower effective diffusion coefficient (Ruthven, 1984).

Table 11: Experimental data for Crank mass transfer model for metabolically inactive adsorbents.

Adsorbents	SS	BB	S&S	Cons	PB	KP
Best-fit values						
Q_t (mg/g)	58.16	53.42	50.21	51.18	27	23.10
k	$2.57x10^{-5}$	$2.4x10^{-4}$	$5.69x10^{-4}$	$3.5x10^{-4}$	$4.54x10^{-5}$	$5.4x10^{-4}$
De (m^2/s)	2.57 $x10^{-13}$	2.4 $x10^{-12}$	5.69 $x10^{-12}$	3.5 $x10^{-12}$	4.54 $x10^{-13}$	5.4 $x10^{-12}$
Goodness of Fit						
R^2	0.9915	0.9879	0.9996	0.9929	0.9765	0.9862
SSE	22.11	28.28	0.9465	16.68	16.63	6.002
Sy.x	2.103	2.378	0.4351	1.667	1.665	1.225
RMSE	1.92	2.171	0.3972	1.544	1.541	1.096

4.3 Effect of Pb(II) concentration on its removal

The effect of adsorbate concentration on the adsorption was investigated by varying the initial concentration of Pb(II) on the metabolically inhibited adsorbents as shown in Figure 4. The results revealed that the percentage of removal of Pb(II) decreased with an increase in Pb(II) concentration as shown in Table 12.

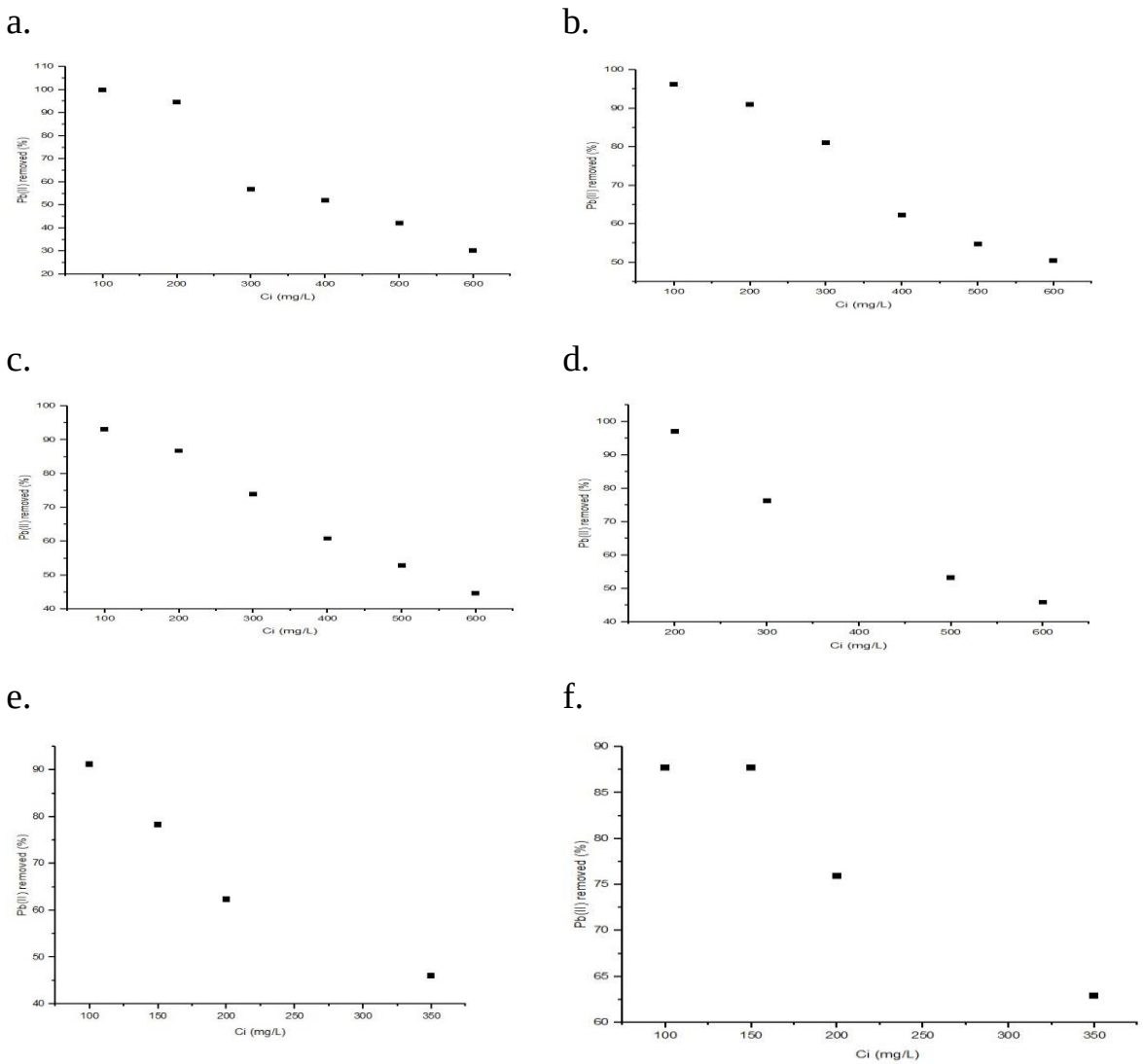

Figure 4: Percentage of Pb(II) removal at different concentrations by a metabolically inhibited (a) SS, (b) BB, (c) S&S, (d) Cons, (e) PB, and (f) KP.

The higher uptake of Pb(II) at low concentration by the adsorbents may be attributed to the availability of more sites on the adsorbent's surface for lesser number of adsorbate species. The decrease in Pb(II) adsorption at higher concentrations suggests lack of available sites on the surface of the adsorbents. This aligns with literature as the adsorption kinetics of the adsorbents agrees with pseudo-second order kinetics which assumes that the rate of adsorption of solute is proportional to the available sites on the adsorbent (Gupta et al., 2021).

Table 12: Percentage of Pb(II) removal

Adsorbents	Initial Pb(II) concentration	Pb(II) removal	Initial Pb(II) concentration	Pb(II) removal
SS	100 mg/L	99.83 %	600 mg/L	30.30 %
BB	100 mg/L	96.23 %	600 mg/L	50.38 %
S&S	100 mg/L	93.06 %	600 mg/L	44.55 %
Cons	200 mg/L	97.02 %	600 mg/L	45.87 %
PB	100 mg/L	91.16 %	350 mg/L	45.93 %
KP	100 mg/L	87.69 %	350 mg/L	62.87 %

4.4 Adsorption isotherm

The results of the isotherm fits for the Langmuir, Two Surface Langmuir, and Freundlich isotherms for the different adsorbents are reported in Appendix B: Figures 11, 12 and 13 as well as Tables 13, 14 and 15, respectively.

The Langmuir isotherm model had an average coefficient of determination (average R^2 = 0.6133), average sum of squared errors (average SSE = 38500.50), average standard error of estimates (average Sy.x = 27.79), and an average root mean square error (average RMSE = 27.55) as presented in Table 13.

Table 13: Langmuir isotherm parameters for the adsorption of Pb(II) by metabolically inactive adsorbents.

Adsorbents	SS	BB	S&S	Cons	PB	KB
Best-fit values						
Q_{max} (mg/g)	141.20	208.50	193.80	220.40	153.20	217.70
K_L (L/mg)	3.68	0.2577	0.0583	0.0245	0.0221	0.0429
R_L	0.0027 – 0.00045	0.037 – 0.0064	0.145 – 0.028	0.290 – 0.064	0.475 – 0.114	0.318 – 0.062
Goodness of Fit						
R^2	0.6483	0.6441	0.6809	0.788	0.3504	0.5682
SSE	15116	52666	40210	26282	35371	61358
Sy.x	18.75	31.82	27.81	25.63	28.68	34.03
RMSE	18.54	31.52	27.54	25.32	28.35	34.03

The adsorption process was relatively well described by the two-surface Langmuir isotherm model which yielded an average coefficient of determination (average $R^2 = 0.7494$), average sum of squared errors (average SSE = 26272.67), average standard error of estimates (average Sy.x = 23.06), and average root mean square errors (average RMSE = 22.57) as presented in Table 14.

Two-surface Langmuir equilibrium isotherm model well described the adsorption of Pb(II) by the metabolically inhibited SS, BB, S&S, PB, and KP. This might be due to the grouping of different adsorption sites into different binding sites which allows a comparably better description of adsorption (Van Veenhuyzen et al.,

2021b). Langmuir equilibrium isotherm model well described the adsorption of Pb(II) by the metabolically inhibited Cons which implies that homogeneous adsorption surfaces (monolayer adsorption) on the adsorbents is involved in the adsorption of Pb(II).

Table 14: Two – surface Langmuir isotherm parameters for the adsorption of Pb(II) by metabolically inactive adsorbents.

Adsorbents	SS	BB	S&S	Cons	PB	KP
Best-fit values						
$Q_{\max 1}$ (mg/g)	72.46	86.07	52.61	$1.401x10^{-10}$	45.82	46.13
$Q_{\max 2}$ (mg/g)	83.83	144.20	156.70	221.40	430.80	223.60
K_{L2} (L/mg)	0.02386	0.03542	0.02166	0.0248	0.001329	0.01491
Goodness of Fit						
Degrees of Freedom	42	51	51	39	42	51
R^2	0.8267	0.8327	0.737	0.7876	0.648	0.6641
SSE	7446	23818	33143	26332	19166	47731
Sy.x	13.31	21.61	25.49	25.98	21.36	30.59
RMSE	13.01	21.20	25.01	25.34	20.87	30.01

The Freundlich isotherm model yielded an average coefficient of determination of (average R^2 = 0.6936), average sum of squared errors (average SSE = 31389), average standard error of estimates (average Sy.x = 25.08), and an average root mean square error (average RMSE = 24.81) as presented in Table 15.

The Freundlich isotherm model best described the adsorption of Pb(II) by the metabolically inhibited SS, BB, PB, and KP when compared with Langmuir isotherm model because Freundlich model takes surface roughness into account whiles Langmuir model works with the assumption that the adsorption should be limited to the formation of a monolayer (Kowanga et al., 2016) and it is also of the assumption that, the number of uniform adsorption sites should finite and lateral interactions between adsorbed species should be absent, and it is likely none of these assumptions apply in biological systems (Igwe and Abia, 2007).

The adsorption intensity $\left(\frac{1}{n}\right)$ for the Freundlich isotherm models for all adsorbents was less than 1 which indicates favourable sorption. Though the sorption process was described poorly by Langmuir isotherm model for all adsorbents in the exception of the Cons and S&S when compared to the two-phase Langmuir and Freundlich isotherm models, the adsorption process was favourable as the separation factor (R_L) was found to be between 0 and 1 (Foo and Hameed, 2010) as presented in Table 13.

The fitting of equilibrium adsorption data to Langmuir and Freundlich isotherm models shows that both homogeneous and heterogeneous adsorption surfaces on the adsorbents were involved in the adsorption of Pb(II).

The maximum adsorption capacity of the metabolically inhibited Cons which was well described by the Langmuir isotherm model was 220.40 mg/g with a bonding energy constant (K_L) of 0.0245 L/mg as presented in Table 12. The maximum adsorption capacities (Q_{max1} and Q_{max2}) of the metabolically inhibited SS, BB, S&S, PB, and KP which were well described by two-surface Langmuir isotherm model were 72.46 mg/g and 83.83 mg/g, 86.07 mg/g and 144.20 mg/g, 52.61 mg/g and 156.70 mg/g, 45.82 mg/g and 430.80 mg/g, and 46.13 mg/g and 223.60 mg/g respectively as presented in Table 13.

Table 15: Freundlich isotherm parameters for the adsorption of Pb(II) by metabolically inactive adsorbents.

Adsorbents	SS	BB	S&S	Con	PB	KP
Best-fit values						
K_f (L/mg)	82.96	89.76	54.55	33.39	21.17	34.39
n	10.11	6.172	4.516	3.295	2.973	2.804
Goodness of Fit						
Degrees of Freedom	43	52	52	40	43	52
R^2	0.8021	0.8264	0.7068	0.7032	0.4957	0.6275
SSE	8504	25686	36942	36805	27459	52938
Sy.x	14.06	22.23	26.65	30.33	25.27	31.91
RMSE	13.90	22.01	26.40	29.96	24.98	31.60

The bonding energy constant (K_{L2}) of the SS, BB, S&S, Cons, PB, and KP by the two-phase Langmuir isotherm model were 0.02386 L/mg, 0.03542 L/mg, 0.02166 L/mg, 0.0248 L/mg, 0.001329 L/mg, and 0.01491 L/mg, respectively.

The highest bonding energy constant was recorded in the bran-based filler bacteria, whiles the lowest bonding energy constant was observed in PB. According to (Del-Bubba et al., 2003), bonding energy constant, K_L is a measure of the affinity of the adsorbate to the adsorbent.

The Freundlich constant (K_f) can provide an evaluation of the amount of adsorbed metal in (mg/kg) at a solution concentration of (1 mg/L) (Welp and Brümmer, 1999). High Freundlich constant (K_f) value indicates high adsorption capacity and vice versa (Kamal, 2020). The K_f value of the metabolically

inhibited SS, BB, S&S, Cons, PB, and KP were 82.96 L/mg, 89.76 L/mg, 54.55 L/mg, 33.39 L/mg, 21.17 L/mg, and 34.39 L/mg, respectively as presented in Table 14. These results indicate that the BB has a high capability to Pb(II) adsorption while PB has a low capability to Pb(II) adsorption. Additionally, the high value of K_f shows lower mobility and higher retention of the Pb(II) (Kamal, 2020), whiles the low value of K_f shows that most of the Pb(II) present in the system are obtainable for transport, chemical processes, and plant uptake (Jalali and Moharrami, 2007).

Based on the highest value of coefficient of determination (R^2) and the lowest sum of squared errors (SSE), standard error of estimates (Sy.x), and root mean square errors (RMSE), the adsorption equilibrium isotherm models could be placed in the following sequence in terms of best – fitting model: Two – surface Langmuir isotherm model > Freundlich isotherm model > Langmuir isotherm model.

Additionally, the mixed-effects model Restricted maximum likelihood (REML) statistical test for the temperature effect on the adsorbents was investigated as presented in Table 15. It was assessed that the temperature range (25°C, 35°C, and 45°C) over which the adsorption experiments were performed did not have a significant effect on the adsorption capacity of the adsorbents (SS, BB, S&S, Cons, PB, and KP) and as a result, thermodynamic analysis are not possible. The implication of this is that the adsorption process on these adsorbents were insensitive to temperature and therefore an industrial adsorption process should be relatively robust for a wide range of operational temperatures.

Table 16: Statistical test for temperature effect.

Adsorbents	Statistical difference in datasets		Matching	
	P value	**Statistically significant (P < 0.05)?**	**Is there significant matching**	**P value**
SS	0.066	No	<0.0001	Yes
BB	0.1376	No	<0.0001	Yes
S&S	0.1671	No	<0.0001	Yes
Con	0.0988	No	<0.0001	Yes
PB	0.2172	No	<0.0001	Yes
KB	0.356	No	<0.0001	Yes

The Langmuir maximum adsorption capacities of several adsorbents are presented in Table 18 for comparison. It is evident that the metabolically inhibited SS, BB, S&S, Cons, PB, KP have comparably high maximum adsorption capacities of 141.20 mg/g, 208.50 mg/g, 193.80 mg/g, 220.40 mg/g, 153.20 mg/g, and 217.70 mg/g, respectively. This characteristic in addition in addition to the low cost of microbial preparation makes it a favorable adsorbent for Pb(II) removal from industrial effluents.

Table 17: Langmuir adsorption capacity for Pb(II) on adsorbents from previous studies.

Adsorbent description	Q_{max} (mg/g)	Reference
Rhodococcus sp. HX-2	88.74	Hu et al., 2020
Streptomyces rimosus	135	Selatnia et al., 2004
Ion imprinted magnetic biosorbent	116.28	He et al., 2019
Magnetic modified vermiculite	70.40	Yao et al., 2016
Magnetic sewage sludge biochar	99.90	Ifthikar et al., 2017

Magnetic sewage sludge biochar	99.90	Ifthikar et al., 2017
Sludge derived biochar	40.80	Zhou et al., 2015
Pyrolyzed sewage sludge	40.30	Rozada et al., 2008
Rawn WAS	143	Hammaini et al., 2007
Raw WAS	307	Van Veenhuyzen et al., 2021b
$ZnCl_2$ activated WAS	274	Van Veenhuyzen et al., 2021b
SS	141.20	This study
BB	208.50	This study
S&S	193.80	This study
Cons	220.40	This study
PB	153.20	This study
KP	217.70	This study

4.5 FTIR analysis

FTIR analysis for functional groups (Presented in Appendix C: Figures 14 to 19) revealed the presence of functional groups in the samples. The wavelength and functional group obtained from the spectra are presented in Table 18 below.

Table 18: FTIR frequency range and functional groups present in the SS, BB, S&S, Cons, PB, and KP.

Wavelength (cm^{-1})	Bond	Functional Group	Adsorbent	Reference
504	C-I	Alkyl halide	Cons, PB	Meenambal et al., 2012
524	C-Br	Alkyl halide	BB, S&S	Meenambal et al., 2012

553	C-Br	Alkyl halide	Cons, PB	Meenambal et al., 2012
544	C-Br	Alkyl halide	SS	Meenambal et al., 2012
606	C-Cl	Alkyl halide	BB	Meenambal et al., 2012
640 - 799	C-Cl	Alkyl halide	Cons, PB	Meenambal et al., 2012
1025	C-N	Amine	Cons, PB	Rushikesh et al., 2018
1034	C-O-C	Ethers	SS	Muruganantham et al., 2009
1050	C-O-C	Ethers	S&S	Muruganantham et al., 2009
1080	C-O-C	Ethers	BB	Muruganantham et al., 2009
1214	C-N	Aliphatic amines	Cons, PB	Rushikesh et al., 2018
1240	C=O	Alkyl ketone	SS, BB, S&S	Deepashree et al., 2013
1406	C=C	Aromatic	PB	Rushikesh et al., 2018
1530	R-OH	Phenol ring	SS	Muthanna et al., 2009
1620	C=C	Alkene	PB	Rushikesh et al., 2018
1528, 1632		Diketones	BB	Deepashree et al., 2013

1530, 1578		Diketones	S&S	Meenambal et al., 2012
1632		Diketones	SS	Deepashree et al., 2013
1640	C=O	Amide	KP	Y. Liu et al., 2016
1745	C=O	Ketone	S&S	
1800	C=O	Anhydride	BB	
2924-2934	R-CH_3	Methyl group	SS, BB, S&S	Deepashree et al., 2013
Circa 3290	O-H	Hydroxyl group	KP, SS, BB, S&S	Deepashree et al., 2013
Circa 3790	O-H Stretching	Alcohol	SS, BB	Salimon et al., 2011

The presence of alkyl halides and phenols was revealed due to the occurrence of peaks at wavelengths of 504 - 799 cm^{-1} and 1019 – 1214 cm^{-1} for both Cons and PB. Aromatic and alkene functional groups were identified in PB microbial strain at wavelengths of 1406 cm^{-1} and 1620 cm^{-1} respectively.

In KP microbial strain, hydroxyl compound was revealed due to the occurrence of the broad peak found at a wavelength of 3298 cm^{-1}. This finding aligns with literature which shows that hydroxyl functional groups are mainly responsible for the adsorption of Pb(II) (Xiaoping & Xiaoning, 2013). The band occurring at 1640 cm^{-1} was attributed to the occurrence of C=O in amide.

The functional groups identified in the SS, BB, and S&S were alkyl halides, ethers, alkyl ketones, diketones, and methyl group at wavelengths of 524 – 544 cm^{-1}, 1034 – 1080 cm^{-1}, 1240 cm^{-1}, 1528 – 1632 cm^{-1}, and 2924 – 2934 cm^{-1} respectively. Hydroxyl compounds and alcohol functional groups were identified in the SS and the BB at wavelengths of 3282 cm^{-1} and

3792 cm^{-1} respectively. NO_2 stretch was identified in both BB and S&S at wavelength of 1398 cm^{-1} respectively. Aromatic and phenol rings were identified in the sewage sludge at wavelengths of 1400 cm^{-1} and 1530 cm^{-1} respectively. Anhydride functional group was identified in the BB at a wavelength of 1800 cm^{-1}. Carboxylic acid was identified at the wavelength of 3276 cm^{-1} in the S&S.

This demonstrated that metabolically inactive Cons, PB, KP, SS, BB, and S&S surfaces contained these active functional groups.

No difference was observed in any of the spectra which shows that the surface characteristics of the adsorbents remain unchanged and oven drying at 74 °C for 24 h did not rupture the cell wall.

4.6 SEM - EDS Analysis

SEM-EDS analysis of the surface morphology and the elemental composition of the metabolically inhibited adsorbents was carried out and the images obtained of the metabolically inhibited SS, BB, S&S, Cons, PB, and KP are shown in Figures 5 and 6 below and the quantitative results are presented in Appendix D: Tables 21 – 26.

The morphology of the metabolically inhibited adsorbents was determined using a scanning electron microscope (SEM). From the results, the surfaces of the metabolically inhibited adsorbents are observed to have uneven and heterogeneous morphologies which may have important effect on the adsorption process (Ge et al., 2016). The surfaces of the adsorbents are rough with irregular crevices, this feature is very dominant in the metabolically inhibited SS as compared to the other adsorbents as shown in Figure 5. Micropores are present in the metabolically inhibited BB and Cons as shown in Figures 5b and d, whiles mesopores are observed in the metabolically inhibited S&S and PB as shown in

Figures 5c and f. Metabolically inhibited KP is mainly characterized with macropores which is presented in Figure 5e.

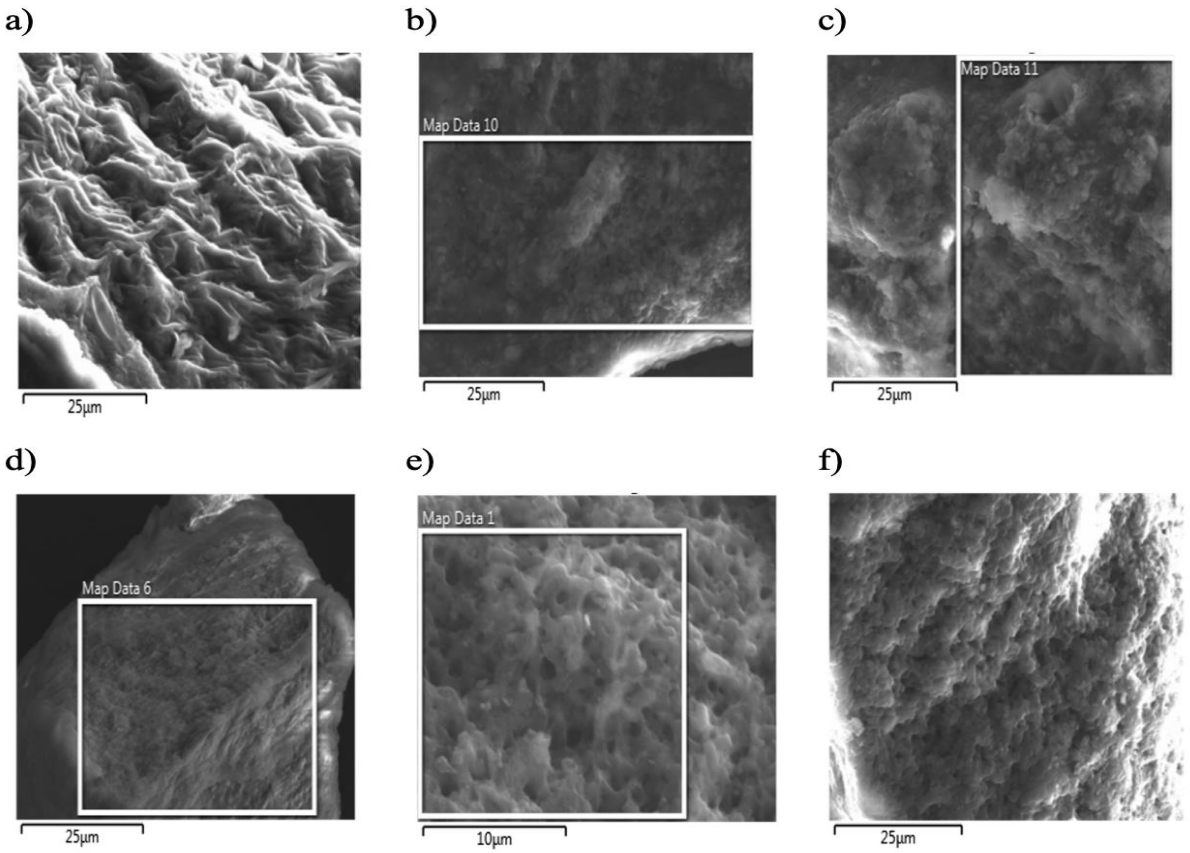

Figure 5: SEM images for a) SS, b) BB, c) S&S, d) Cons, e) KP, f) PB.

Similar observation was reported by Anisuzzaman et al. (2015) in their study on commercial activated carbon adsorbents modified for the removal of phenol. According to Pezoti et al. (2016), the cavities on the surface of the adsorbents serves as channels for Pb(II) in the adsorbate system thereby providing access to the micro, meso, and macropores where surface adsorption and chemical interactions can occur with the surface functional groups on the adsorbent active sites. The surface alterations observed in the SEM of the metabolically inhibited adsorbents may be due to the effect of the sorption processes on the adsorbents as the aqueous adsorbate interacts with the adsorbents. This observation was also reported by Asuquo et al. (2016) in the study of commercial activated carbon adsorbent (CGAC) for Pb(II) and Cd(II) removal from aqueous solutions.

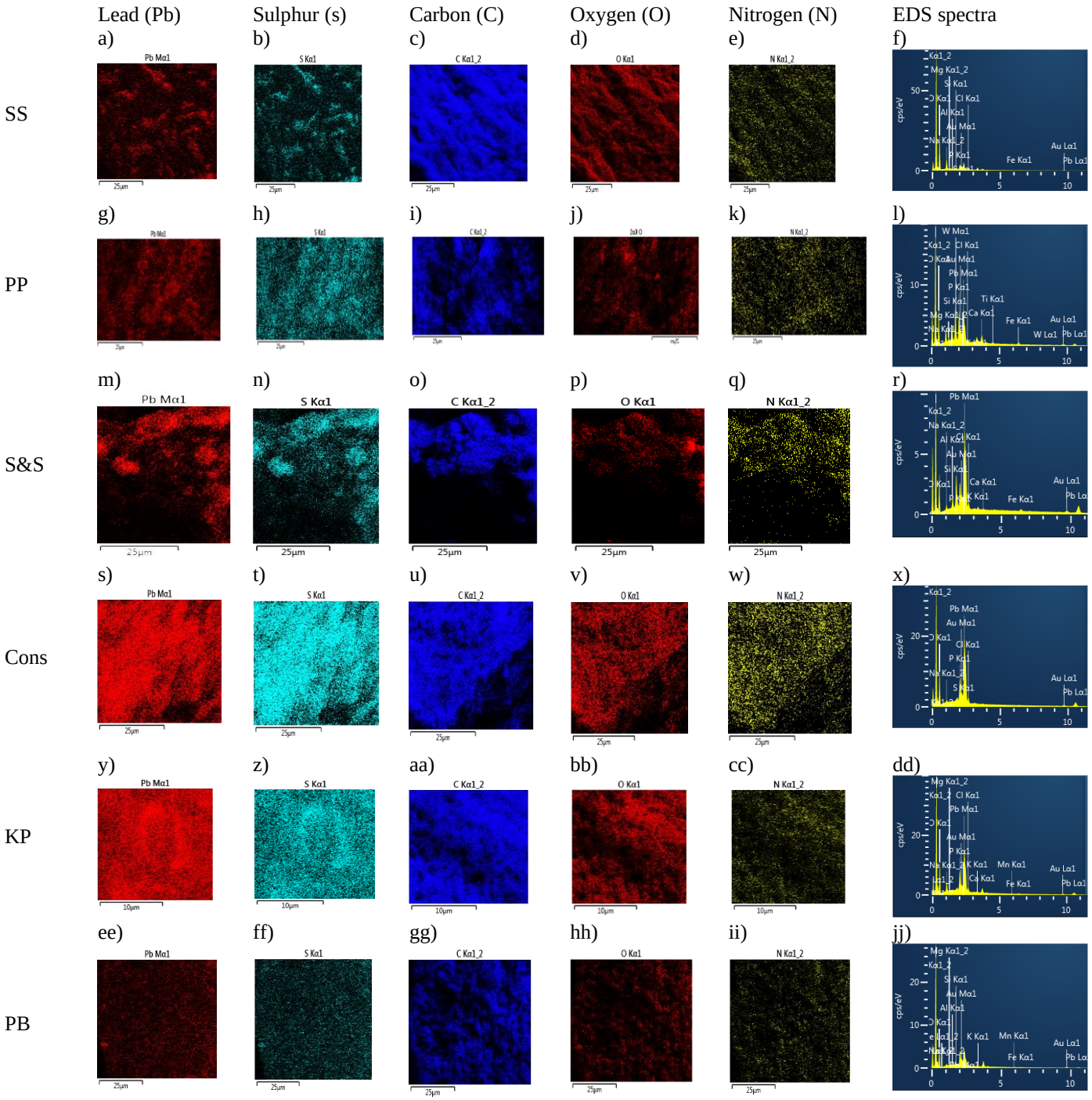

Figure 6: EDS Maps and corresponding EDS spectra on a) – f) SS, g) – l) BB, m) – r) S&S, s) – x) Cons, y) – dd) KP, ee) – jj) PB (indicated on the left). The maps represent Pb, S, C, O, N and the EDS spectra (as indicated at the top).

The EDS analyses of the metabolically inhibited SS, BB, S&S, Cons, KP, and PB after Pb(II) sorption (Figure 6) lends credence to the observation that the metabolically inhibited adsorbents were able to remove Pb from the aqueous

solutions, as it clearly demonstrates the fate of the Pb(II) on the surface of the adsorbents. In addition, the EDS spectrum for each metabolically inhibited adsorbent clearly shows the peaks for Pb confirming their existence on the surface of the adsorbents after sorption was carried out. This observation was also reported by Van Veenhuyzen et al. (2021b), in their study of high capacity Pb(II) adsorption characteristics onto raw-and chemically activated sewage sludge. Erdem et al. (2013) also reported this observation in their study on the accumulation of Pb(II) onto activated carbon derived from waste biomass, where the occurrence of Pb(II) peak on the EDS spectrum was used to prove the accumulation of Pb(II) on the adsorbent.

From the qualitative analysis of the respective EDS maps, it can further be seen that significant similarities between the distributions of the S and the Pb could be observed, indicating that there are likely strong interactions between these species on the surfaces. This observation is consonant with results observed by Hamilton et al. (2020) in which it was observed that Pb chemically interacts during adsorption forming strong surface complexes. In addition, it is noteworthy that limited similarities between Pb and either C, O or N were observed, likely due to limited interactions between these species.

4.7 Regeneration and reusability

Adsorbents regenerated using 0.1 M HNO_3 recorded an efficiency of 72.35 %, 68.62 %, 69.73 %, 69.58 %, 60.99 %, and 72.38 % in Pb(II) recovery by the metabolically inhibited SS, BB, S&S, Cons, PB, and KP respectively during the first desorption cycle.

In the second desorption cycle, metabolically inhibited SS, BB, S&S, Cons, PB, and KP showed desorption efficiencies of 14.03 %, 2.32 %, 3.35 %, 0.87 %, 0.74 %, and 4.94 %, respectively.

The amount of Pb(II) desorbed in the first desorption cycle by the metabolically inhibited SS, BB, S&S, Cons, PB, and KP were 64.97 mg/g, 70.64 mg/g, 71.46 mg/g, 66.76 mg/g, 50.16 mg/g, and 79.53 mg/g respectively. In the second desorption cycle, 13.45 mg/g, 3.26 mg/g, 4.08 mg/g, 2.11 mg/g, and 31.87 mg/g of Pb(II) was desorbed by the metabolically inhibited SS, BB, S&S, Cons, PB, and KP respectively as shown in Table 22.

The adsorption capacity for the metabolically inhibited SS, BB, S&S, PB, and KP after the second cycle of regeneration decreased by 66.95 %, 75.53 %, 67.47 %, 18.93 %, and 1.19 % respectively as shown in Table 23. This observation aligns with literature as Van Veenhuyzen et al. (2021b) reported a 44 % loss in adsorption capacity as a result of acid hydrolysis of binding sites. According to Tao et al. (2020), the drop in adsorption capacity might arise from the inability of the eluent to overcome high affinity between binding sites and Pb(II). In contrast, the metabolically inhibited consortium had a 63.23 % increase in adsorption capacity.

Table 19: Desorption efficiency and amount of Pb(II) desorbed by metabolically inhibited adsorbents.

Adsorbents	Pb(II) desorbed (%) 1st cycle	Q_d (mg/g)	Pb(II) desorbed (%) 2nd cycle	Q_d (mg/g)
SS	72.35	64.97	14.03	13.45
BB	68.62	70.64	2.32	3.26
S&S	69.73	71.46	3.35	4.08
Cons	69.58	66.76	0.87	2.11
PB	60.99	50.16	0.74	2.43
KP	72.38	79.53	4.94	12.32

Table 20: Adsorption capacity of metabolically inhibited adsorbents before and after regeneration.

Adsorbents	Q_e before regeneration	Q_e after regeneration
SS	89.80 mg/g	29.68 mg/g
BB	102.93 mg/g	25.19 mg/g
S&S	102.47 mg/g	33.33 mg/g
Cons	95.95 mg/g	156.62 mg/g
PB	82.24 mg/g	66.67 mg/g
KP	109.88 mg/g	108.57 mg/g

These results clearly indicate the potential of these biosorbents as low cost adsorbents not only for the effective removal of aqueous Pb(II) from solution, but also for the concentration and recovery of Pb(II) thereby facilitating the reuse of this valuable resource.

5. Conclusions

This work dealt with the removal of Pb(II) from aqueous solution using a metabolically inactive sewage sludge (SS), bran-based filler bacteria (BB), salt-and-starch filler bacteria (S&S), Pb(II) resistant consortium (Cons), Pb(II) resistant *P. bifermentans* (PB), and Pb(II) resistant *K. pneumoniae* (KP) as biosorbents. It was found that oven drying the adsorbents at 74 °C for 24 h successfully inhibited the metabolic activity without rupturing the cell wall.

Metabolically inactive SS, BB, S&S, Cons, PB, and KP removed 55.35 mg/g, 54.60 mg/g, 50.63 mg/g, 54.44 mg/g, 27.39 mg/g, and 23.10 mg/g of Pb(II) in 3 h, respectively. It was found that a passive process was responsible for Pb(II) removal from the solution as metabolic activity was not detected using MTT. Black or grey precipitate was not evident in the 14 h period, which indicates that neither PbS nor Pb (0) was formed.

FTIR spectroscopy indicated the adsorption of Pb(II) onto functional groups (Alkyl halides, amine, aliphatic amines, aromatic ring, alkene, amide, hydroxyl compound, ethers, alkyl ketone, phenol ring, diketones, methyl group, alcohol, NO_2 stretch, and carboxylic acid) as being present on the surface of the adsorbents, with no change observed for the adsorbents before or after drying, or after adsorption. This indicates that the surfaces of the adsorbents remained consistent even after the drying process was completed, while the surface species remained unaffected by the adsorption process.

An increase in pH which was observed in the metabolically inhibited consortium, *P. bifermentans*, sewage sludge, bran-based-filler bacteria, and salt-and-starch-based filler bacteria might have been as a result of the electrostatic attraction between the negatively charged surface of the adsorbents and the positively charged Pb(II) ions which results in an increase in adsorption efficiency. The decrease in pH as observed in *K. pneumoniae* is likely due to the release of

protons from the surface of the bacteria because of cation exchange processes in which the H^+ions are displaced by the Pb(II) ions on the surface of the adsorbent.

Additionally, two – phase pseudo – first – order kinetics satisfactorily predicted the behavior of the sorption processes as compared to pseudo – first – order and pseudo – second – order kinetics. This might be because of the separation of fast and slow adsorption rates into separate compartments, thereby allowing for better representation of a heterogeneous surface. It was also found that pseudo – second - order kinetic model represents the data better as compared to pseudo – first – order kinetic model which indicates an abundance of adsorption sites relative to Pb(II) ions in the solution.

Pseudo – first – order kinetic model, two – phase pseudo – first – order, and pseudo – second – order kinetic model was used to compare the goodness of fit to describe the adsorption kinetics of Pb(II). Two – phase pseudo – first – order kinetics compared to the other kinetic models is considered as the best model for describing Pb(II) adsorption kinetics as it has the highest coefficient of determination (R^2) and the lowest sum of squared errors (SSE), standard error of estimates (Sy.x), and root mean square errors (RMSE).

The order of the values of diffusion coefficients for the adsorbents using Crank mass transfer model was found as follows: S&S > KP > PB > Cons > SS BB bacteria. Crank mass transfer model shows that external mass transfer is the main mechanism of Pb(II) removal due to the high molecular diffusivity of Pb(II) as compared to the diffusion coefficients of the metabolically inhibited adsorbents.

The higher uptake of Pb(II) at low concentration and the decrease in Pb(II) adsorption at higher concentrations suggests availability of more sites on the adsorbent's surface for lesser number of adsorbate species and lack of available sites on the surface of the adsorbents respectively.

Results showed that the BB bacteria had the lowest mobility and the highest sorption capacity while PB had the highest mobility and the lowest sorption capacity. Freundlich constant (K_f) related to sorption capacity could place according to the following sequence: BB > SS > S&S > KP > Cons > PB.

The highest bonding energy constant (K_{L2}) was recorded in the BB while the lowest bonding energy constant was recorded in PB. Bonding energy constant (K_{L2}) which is a measure of the affinity of the adsorbate to the adsorbent could place according to the following sequence: BB > Cons > SS > S&S > KP > PB.

Langmuir isotherm model, two – surface Langmuir isotherm model, and Freundlich isotherm model were used to compare the goodness of fit to describe the adsorption of Pb(II). Two – surface Langmuir isotherm model compared to the other models is considered as the best model for describing Pb(II) adsorption since it has given the highest value of coefficient of determination (R^2) and the lowest sum of squared errors (SSE), standard error of estimates (Sy.x), and root mean square errors (RMSE).

It was assessed from the statistical test for temperature effect on the adsorbents that the temperature range over which the adsorption experiments were performed did not have a significant effect on the adsorption capacity of the adsorbents and as a result, thermodynamic analysis are not possible.

SEM and EDS analyses of the metabolically inhibited adsorbents gave insight into the morphology and chemical nature of the adsorbents. The morphology of the adsorbents showed that the surface of the metabolically inhibited adsorbents was rough, coarse with considerable pore volume and irregular crevices. The results from the EDS analyses indicated the presence of Pb on the surface of the metabolically inhibited adsorbents confirming the adsorbents were able to remove Pb(II) from the aqueous systems.

Metabolically inhibited SS, BB, S&S, Cons, PB, KP demonstrated 72.35 %, 68.62 %, 69.73 %, 69.58 %, 60.99 %, and 72.38 %, respective, in Pb(II) recovery after the first cycle. A decrease in adsorption capacity of the adsorbents was observed after the second cycle of Pb(II) recovery in the exception of the metabolically inhibited consortium which demonstrated 63.23 % increase in adsorption capacity.

Overall the study provides strong evidence for the potential of these biosorbents for the removal of Pb(II) from aqueous solution as well as the recovery of Pb(II) for subsequent reuse.

It is recommended that more detailed study be done to elucidate the mechanisms of adsorption for the respective adsorbent as required for more effective scaling. In addition, optimisation studies could be done to assess the optimal operational conditions for adsorption for the different adsorbents.

References

Abatenh, E., Gizaw, B. Tsegaye, Z., & Wassie, M. (2017). "The role of microorganisms in bioremediation." Open Journal of Environmental Biology, 2(1), 38-46.

Abbaszadeh, S., Alwi, S. R., Webb, C., Ghasemi, N., & Muhamad, I. I. (2016). "Treatment of lead-contaminated water using activated carbon adsorbent from locally available papaya peel biowaste." Journal of Cleaner Production, 118, 210-222.

Abu-Qudais, H., & Moussa, H. (2004). "Removal of Heavy Metals from Wastewater by Membrane Processes: A Comparative Study." Desalination, 164, 105-110. doi:10.1016/S0011-9164(04)00169-9.

Ahalya, N., Ramachandra, T. V., & Kanamadi, R. D. (2003). "Biosorption of heavy metals." Research Journal of Chemistry and Environment, 7(4), 71-79.

Ahluwalia, S. S., & Goyal, D. (2007). "Microbial and plant-derived biomass for removal of heavy metals from wastewater." Bioresource Technology, 98(12), 2243-2257.

Ahn, S., Oh, J., & Sohn, K. (2001). "Mechanistic Aspects of Nitrate Reduction by Fe(0) in Water." Journal of the Korean Chemical Society, 45.

Ali, H., & Khan, E. (2018). "What are heavy metals? Long-standing controversy over the scientific use of the term 'heavy metals' – proposal of a comprehensive definition." Toxicological and Environmental Chemistry, 100, 6-19. doi:10.1080/02772248.2017.1413652.

Amarasinghe, B. M. W. P. K., & Williams, R. A. (2007). "Tea waste as a low-cost adsorbent for the removal of Cu and Pb from wastewater." Chemical Engineering Journal, 132(1-3), 299-309.

American Water Works Association; James Edzwald (1999 & 2011). Water Quality & Treatment: A Handbook on Drinking Water, Sixth Edition.

Anisuzzaman, S. M., Joseph, C. G., Taufiq-Yap, Y. H., Krishnaianh, D., & Tay, V. V. (2015). "Modification of commercial activated carbon for the removal of 2,4-dichlorophenol from simulated wastewater." Journal of King Saud University-Science, 27(4), 318-330.

Anwar, J., Shafique, U., Salman, M., Dar, A., & Anwar, S. (2010). "Removal of Pb(II) and Cd(II) from water by adsorption on peels of banana." Bioresource Technology, 101(6), 1752-1755.

Asuqo, E., Alastair, M., Petrus, N., Siperstein, F., & Xiaolei, F. (2016). "Adsorption of Cd(II) and Pb(II) ions from aqueous solutions using mesoporous activated carbon adsorbent: Equilibrium, kinetics, and characterization.

Ateia, M, Yoshimura, C and Nasr, M (2016) "In-situ biological water treatment technologies for environmental remediation: a review" J Bioremed Biodeg, 7(348), 2.
ATSDR (1999) Toxicological profile for petroleum hydrocarbons (PHC).
Background document for development of WHO Guidelines for Drinking-water Quality (2011) Lead in Drinking-water, link.
Bala, S, Garg, D, Thirumalesh, BV, Sharma, M, Sridhar, K, Inbaraj, BS and Tripathi, M (2022) "Recent Strategies for Bioremediation of Emerging Pollutants A Review for a Green and Sustainable Environment" Toxics, 10(8), 484, DOI: link.
Barakat, MA (2011) "New trends in removing heavy metals from industrial wastewater" Arabian Journal of Chemistry, Volume 4, Issue 4, 361-377, ISSN 1878-5352, link.
Bayuo, J, Abukari, M and Pelig-Ba, K (2020) "Desorption of chromium (VI) and lead (II) ions and regeneration of the exhausted adsorbent" Applied Water Science, 10(7), DOI: 10.1007/s13201-020-01250-y.
Berkessa, YW, Mereta, ST and Feyisa, FF (2019) "Simultaneous removal of nitrate and phosphate from wastewater using solid waste from factory" Appl Water Sci 9, 28, link.
Bharathi, KS and Ramesh, ST (2013) "Removal of dyes using agricultural waste as low-cost adsorbents" A review. Appl. Water Sci., 3:773–790, doi: 10.1007/s13201-013-0117-y.
Bilal, S, Ali, MS, Farid, M, Ahsan, MF, Tauqeer, MH, Iftikhar, U, Hannan, F and Bharwana, SA (2013) "Heavy metal pollution, a global problem and its remediation by chemically enhanced phytoremediation: A Review" Journal of Biodiversity and Environmental Science, 3, 12 – 20, ISSN: 2220-6663.
Blair, C and Ursache, A (2011) "A bidirectional model of executive functions and self-regulation," Handbook of Self-Regulation: Research, Theory, and Applications. Vol. 2, Guilford Press; 300 – 20.
Bolster, CH and Hornberger, GM (2007) "On the use of linearized Langmuir equations" Soil Sci. Soc. Am. J. 71, 1796 – 1806.
Boyd, GE, Adamson, AW and Myers, LS (1947) "The Exchange Adsorption of Ions from Aqueous Solutions by Organic Zeolites. II. Kinetics" Journal of the American Chemical Society 69(11), 283Brink, H, Hörstmann, C and Feucht, C (2019) “Microbial Pb(II) Precipitation: Minimum Inhibitory Concentration and Precipitate Identity” Chemical Engineering Transactions, 74, 1453–1458 doi: 10.3303/CET1974243.
Brink, HG, Lategan, M, Naudé, K and Chirwa, E (2017) "Lead removal using industrially sourced consortia: influence of lead and glucose concentrations" Chemical Engineering Transactions, 57, 409 – 414, DOI: 10.3303/CET1757069.

Brown, MJ, and Margolis, S (2012) "Lead in Drinking Water and Human Blood Lead Levels in the United States" Centers for Disease Control and Prevention, National Center for Environmental Health, 61.
Brunekreef, B (1986) "Childhood Exposure to Environmental Lead, MARC Report 34, London" Monitoring and Assessment Research Centre, King's College, University of London.
Carpio, IE, Mangadlao, JD, Nguyen, HN, Advincula, RC and Rodrigues, DF (2014) "Graphene oxide functionalized with ethylenediamine triacetic acid for heavy metal adsorption and anti-microbial applications" Carbon, 77: 289 – 301.
Cengeloglu, Y, Tor, A, Ersoz, M and Arslan, G (2006) "Removal of nitrate from aqueous solution by using red mud" Sep Purif Technol 51:374 – 378.
Cesur, H and Baklaya, N (2007) "Zinc removal from aqueous solution using an industrial by-product phosphogypsum" Chemical Engineering Journal, 131(1-3), 203 – 208, DOI: 10.1016/j.cej.2006.11.010.
Chen, HJ, Lin, YZ, Fanjiang, JM and Fan, C (2013) "Microbial community and treatment ability investigation in AOAO process for the optoelectronic wastewater treatment using PCR-DGGE biotechnology" Biodegradation, 24(2), 227 - 243.
Chetty, S and Pillay, L (2019) "Assessing the influence of human activities on River health: A case for two South African rivers with differing pollutant sources" Environ. Monit. Assess., 191, 168, DOI: 10.1007/s10661-019-7308-4.
Chisolm, JJ (1971) "Lead Poisoning" Scientific American, Vol.224, 17 - 23.
Cosgrove, E, Brown, MJ, Madigan, P et al. (1989) "Childhood lead poisoning: case study traces source to drinking water" Journal of environmental health, 52, 346.
Couto, N, Rasmussen, FJ, Jensen, PE, Højrup, M, Rodrigo, AP and Ribeiro, AB (2014) "Suitability of oil bioremediation in an Arctic soil using surplus heating from an incineration facility" Environmental Science and Pollution Research, 21(9), 6221–6227. doi:10.1007/s11356-013-2466-3.
Dai, Y, Du, C, Yu, H, Zhang, D and Tanaka, S (2016) "Effect of contact time, solution pH, dosage of adsorbent, and regeneration on adsorption behavior of lead using nitric acid treated carbon material" In: Fresenius Environmental Bulletin 25(9); 3493 – 3506. ISSN: 10184619.
Davidson, A, Binks, S and Gediga, J (2016) "Lead industry life cycle studies: environmental impact and life cycle assessment of lead battery and architectural sheet production" The International Journal of Life Cycle Assessment, 21, DOI: 10.1007/s11367-015-1021-5.
Davis, TA, Volesky, B and Mucci, A (2003) "A review of the biochemistry of heavy metal biosorption by brown algae" Water research, 37(18): 4311 – 30.

Debnath, B, Singh, WS and Manna, K (2019) “Sources and toxicological effects of lead on human health” Indian Journal of Medical Specialities, 10, DOI: 66.10.4103/INJMS.INJMS_30_18.
Deepashree, CL, Komal, KJ, Prasad, AGD, Zarei, M and Gopal, S (2013) “FTIR Spectroscopic Studies on Cleome Gynandra-Comparative Analysis of Functional Group before and after Extraction” Romanian Journal of Biophysics, 22, 137-143.
Dehghani, SAM, Hosseynifar, A, Jahed, V and Mousavi, H Z (2010) “Removal of lead from aqueous solution using waste tire rubber ash as an adsorbent” URL: https://doi.org/10.1590/S0104-66322010000100007.
Department of Water Affairs (2013) Revision of general authorisations in terms of section 39 of the national water act, 1998, (Act no. 36 of 1998) Government Gazette South Africa.
De la Noue, J, Laliberte, G and Proulx, D (1992) “Algae and wastewater” J. Appl. Phycol. 4, 247 – 254.
Del-Bubba, M, Arias, CA and Brix, H (2003) “Phosphorus adsorption maximum of sands for use as media in subsurface flow constructed reed beds as measured by the Langmuir isotherm” Water Research, 37 (14), 3390 – 3400.
Demirbas, A (2008) “Heavy metal adsorption onto agro-based waste materials: a review” Journal of hazardous materials, 157(2-3): 220 – 9.
Demirbas, E, Kobya, M and Konukman, AES (2008) “Error Analysis of equilibrium studies for the almond shell activated carbon adsorption of Cr (VI) from aqueous solutions” Journal of Hazardous Materials, (1 – 3): 787 – 794.
Department for Environment, Food and Rural Affairs, DEFRA (2009) Soil strategy for England supporting evidence paper.
Department of National Health and Welfare (1992). Guidelines for Canadian drinking water quality: supporting documentation, Lead Ottawa, Canada.
Dixit, R, Wasiullah-Malaviya, D, Pandiyan K, Singh, UB, Sahu, A, Shukla, R, Singh, BP, Rai, JP, Sharma, PK, Lade, H and Paul, D (2015) “Bioremediation of heavy metals from soil and aquatic environment” An overview of principles and criteria of fundamental processes Sustain, 7, 2189 – 2212, DOI:10.3390/su7022189.
Do, D (1998) Adsorption analysis: Equilibria and kinetics, Imperial College Press, London
DWS, Directorate Water Resource Planning Systems: Water Quality Planning (2011) Planning Level Review of Water Quality in South Africa, Sub-series No.WQP 2.0, Department of Water Affairs; Pretoria, South Africa.
Eccles, H (1999) "Treatment of metal-contaminated wastes: why select a biological process?" Trends Biotechnol. 17(12), 462-5, DOI: 10.1016/s0167-7799(99)01381-5. PMID: 10557157.
Environmental Canada (2003) Environmental indicator series. URL: http://www.ec.gc.ca/soer.ree. Accessed Jan 27, 2023.

Environmental Security Technology Certification Program (ESTCP) (2005) Bioaugmentation for Remediation of Chlorinated Solvents: Technology Development Status and Research Needs.
EPA (2000) Nutrient criteria technical guidance manual-rivers and streams, EPA-822-B-00-002, Washington DC.
Ewecharoen, A, Thiravetyan, P, Wendel, E and Bertagnolli, H (2009) "Nickel adsorption by sodium polyacrylate-grafted activated carbon" Journal of hazardous materials, 171(1-3): 335 – 9.
Esalah, JO, Weber, ME and Vera, JH (1999) "Removal of lead from aqueous solutions by precipitation with sodium di-(n-octyl) phosphinate" Sep. Purif. Technol., 18, 25 – 36.
Ezzati, R (2019) "Derivation of pseudo-first-order, pseudo-second-order and modified pseudo-first-order rate equations from Langmuir and Freundlich isotherms for adsorption" Chem. Eng. J., 392, 123705.
Fenglian, F and Wang, Q (2011) "Removal of heavy metal ions from wastewaters: A review" Journal of Environmental Management, Volume 92, Issue 3, 407-418, ISSN 0301-4797, DOI: https://doi.org/10.1016/j.jenvman.2010.11.011 https://www.sciencedirect.com/science/article/pii/S0301479710004147.
Fewtrell, LJ, Pruss-Ustun, A, Landrigan, P and Ayuso-Mateos, JL (2004) "Estimating the Global Burden of Disease of Mild Mental Retardation and Cardiovascular Diseases from Environmental Lead Exposure" Environmental Research, Vol. 94, No. 2, 120-133, DOI: http://dx.doi.org/10.1016/S0013-9351(03)00132-4.
Foo, KY and Hameed, BH (2010) "Insights into the modeling of adsorption isotherm systems" Chem Eng J 156, 2 – 10.
Freundlich, HMF (1906) "Over the adsorption in solution" Z. Phys. Chem., 57, 385 – 470.
Gagnon, V, Chazarenc, F, Kõiv, M and Brisson, J (2012) "Effect of plant species on water quality at the outlet of a sludge treatment wetland" Water Res 46: 5305 - 5315.
Garg, SK, Tripathi, M and Srinath, T (2012) "Strategies for chromium bioremediation of tannery effluent" Reviews of Environmental Contamination and Toxicology Volume 217, 75-140.
Gawande, SM, Belwalkar, NS and Mane, AA (2017) "Adsorption and its Isotherm – Theory" International Journal of Engineering Research, 6(6), 312.
Ge, X, Wu, Z, Yan, Y, Cravotto, G and Ye, B (2016) "Microwave-assisted modification of activated carbon with ammonia for efficient pyrene adsorption" Journal of Industrial and Engineering Chemistry.
Goyal, P, Sharma, P, Srivastava, S and Srivastava, MM (2008) "Saraca indica leaf powder for decontamination of Pb: Removal, recovery, adsorbent characterization and equilibrium modeling" International Journal of Environmental Science and Technology, 5(1); 27 – 34. ISSN: 17352630.

Gray, JS (2002) "Biomagnification in marine systems: the perspective of an ecologist" Mar Pollut Bull., 45(1-12), 46-52, DOI: 10.1016/s0025326x(01)00323-x, PMID: 12398366.
Gil, A and Grange, P (1996) "Application of the Dubinin – Radushkevich and Dubinin - Astakhov equations in the characterization of microporous solids" Colloids Surf. A Physicochem. Eng. Asp., 113, 39 – 50.
Gupta, A, Sharma, V, Sharma, K, Kumar, V, Choudhary, S, Mankotia, P, Kumar, B, Mishra, H, Moulick, A, Ekielski, A and Mishra, PK (2021) "A Review of Adsorbents for Heavy Metal Decontamination: Growing Approach to Wastewater Treatment" Materials (Basel), 14(16):4702, doi: 10.3390/ma14164702.
Gupta, A, Yunus, M., Sankararamakrishnan, N., 2013. Chitosan- and Iron–Chitosan-Coated Sand Filters: A Cost-Effective Approach for Enhanced Arsenic Removal. Ind. Eng. Chem. Res. 2013;52:2066 – 2072. doi: 10.1021/ie302428z.
Gupta, VK and Ali, I (2004) "Removal of lead and chromium from wastewater using bagasse fly ash – a sugar industry waste" J. Coll. Inter Sci. 271 (2), 321 – 328.
Guo, X and Wang, J (2019) "A general kinetic model for adsorption: theoretical analysis and modelling" J. Mol. Liq., 288, 111100.
Hadad, HR, Maine, MA and Bonetto, CA (2006) "Macrophyte growth in a pilot-scale constructed wetland for industrial wastewater treatment" Chemosphere 63: 1744 - 1753.
Hammaini, A, Gonzalez, F, Ballester, ML and Mun˜oz, JA (2007) "Biosorption of heavy metals by activated sludge and their desorption characteristics" J. Environ. Manag. 84, 419 – 426.
Hashem, MA, Nur-A-Tomal, MS, Mondal, NR and Rahman, MA (2017) "Hair burning and liming in tanneries is a source of pollution by arsenic, lead, zinc, manganese, and iron" Environ. Chem. Lett., 15, 501 - 506, 10.1007/s10311-017-0634-2.
Hashim, MA, Mukhopadhyay, S, Sahu, JN and Sengupta, B (2011) "Remediation technologies for heavy metal contaminated groundwater" J Environ Manage.; 92(10):2355-88. DOI: 10.1016/j.jenvman.2011.06.009. PMID: 21708421.
He, Y, Wu, P, Xiao, W, Li, G, Yi, J, He, Y, Chen, C, Ding, P and Duan, Y (2019) "Efficient removal of Pb(II) from aqueous solution by a novel ion imprinted magnetic biosorbent: Adsorption kinetics and mechanisms" PLoS One.;14(3):e0213377. doi: 10.1371/journal.pone.0213377. PMID: 30917141; PMCID: PMC6437713.
Hellmann (1970) "Absorption of heavy metals by suspended solids in the Rhine River" Deutsche Gewasserkundliche Mitteilungen, v. 14, no. 2, 42 - 47; English abs. available in Chern. Abs., v. 73, no. 48360b.
Ho, YS and McKay, G (1999) "Pseudo-second order model for sorption processes" Process Biochem 34:451– 465.

Horsfall, M. Jnr and Spiff, AI (2005) "Effects of temperature on the sorption of Pb2+ and Cd2+ from aqueous solution by Caladium bicolor (Wild Cocoyam) biomass" Elect J. Biotech. 8(2), 43 – 50.
Hörstmann, C, Brink, HG and Chirwa, EMN (2020) "Pb(II) Bio-Removal, Viability, and Population Distribution of an Industrial Microbial Consortium: The Effect of Pb(II) and Nutrient Concentrations" Sustainability, p.2511.
Hörstmann, C, Naidoo, S, Brink, H and Chirwa, E (2020) "Microbial Pb(II) Precipitation: Yeast Extract Autolyzed from Saccharomyces Cerevisiae as a Sustainable Growth Substrate" Chemical Engineering Transactions, 79, 421–426 doi: 10.3303/CET2079071.
Hu, X, Cao, J, Yang, H, Li, D, Qiao, Y, et al., (2020) "Pb^(2+) biosorption from aqueous solutions by live and dead biosorbents of the hydrocarbon-degrading strain Rhodococcus sp. HX-2" PLOS ONE 15(1).
Huang, Y, Zeng, X, Guo, L, Lan, J and Cao, D (2018) "Heavy metal ion removal of wastewater by zeolite-imidazolate frameworks" Separation and Purification Technology, 194: 462 – 9.
Hussain, A, Madan, S and Madan, R (2021) "Removal of Heavy Metals from Wastewater by Adsorption" IntechOpen, DOI: 10.5772/intechopen.95841.
Hyndman, RJ and Athanasopoulos, G (2018) Forecasting: principles and practice, OTexts.
Ifthikar, J, Wang, T, Khan, A, Jawad, A, Sun, T, Jiao, X, Chen, Z, Wang, J, Wang, Q, Wang, H and Jawad, A (2017) "Highly efficient lead distribution by magnetic sewage sludge biochar: sorption mechanisms and bench applications" Bioresour. Technol., 238, 399 – 406.
Igwe, JC and Abia, AA (2007) "Equilibrium sorption isotherm studies of Cd(II), Pb(II) and Zn(II) ions detoxification from wastewater using unmodified and EDTA-modified maize husk" Electron Journal of Biotechnology, 10: 536 – 548.
ILA (2019). Lead production statistics. URL: https://ila-lead.org/resources/lead-production-statistics/
Iloms, E, Ololade, O, Ogola, H and Selverajan, R (2020) "Investigating Industrial Effluents Impact on Municipal Wastewater Treatment Plant in Vaal, South Africa" International Journal of Environmental Research and Public Health, 17, 1 – 18
Jae-Wook Lee, Seung-Phil Choi, Ramesh Thiruvenkatachari, Wang-Geun Shim, Hee Moon (2006) "Submerged microfiltration membrane coupled with alum coagulation/powdered activated carbon adsorption for complete decolorization of reactive dyes" Water Research, Volume 40, Issue 3, 435-444, ISSN 0043-1354, https://doi.org/10.1016/j.watres.2005.11.034.
Jakubowski, M (2011) "Low-level environmental lead exposure and intellectual impairment in children – The current concepts of risk assessment" Int J Occup Med Environ Health;24:1-7.

Jalali, M and Moharrami, S (2007) "Competitive adsorption of trace elements in calcareous soils of western Iran" Geoderma, 140(1 – 2), 156 – 163.
Jamwal, A, Phulia, V, Saxena, N, Chadha, NK, Muralidhar and Prusty, A (2013) "Technologies in aquatic bioremediation" Freshwater Ecosystem and Xenobiotics, 65 - 91.
Janyasuthwiong, S and Rene, ER (2017) "Bioprecipitation – A Promising Technique for Heavy Metal Removal and Recovery from Contaminated Wastewater Streams" MOJ Civil Eng., 2(6), 191 – 193.
Jeong, SW, Kim, HK, Yang, JE and Choi, YJ (2019) "Removal of Pb(II) by Pellicle-Like Biofilm-Producing Methylobacterium hispanicum EM2 Strain from Aqueous Media" Water, 11, 2081. https://doi.org/10.3390/w11102081.
Jiang, Z, Jiang, L, Zhang, L, Su, M, Tian, D, Wang, T, … Li, Z (2019) "Contrasting the Pb(II) and Cd(II) tolerance of Enterobacter sp. via its cellular stress responses" Environmental Microbiology.
Kafilzadeh, F, Afrough, R, Johari, H and Tahery, Y (2012) "Range determination for resistance/tolerance and growth kinetic of indigenous bacteria isolated from lead-contaminated soils near gas stations (Iran)" European Journal of Experimental Biology, 2(1), 62 – 69.
Kajjumba, GW et al., (2018) Modelling of Adsorption Kinetic Processes—Errors, Theory and Application, in S. Edebali (ed.), Advanced Sorption Process Applications, IntechOpen, London. 10.5772/intechopen.80495.
Kamal, HK (2020) "Copper adsorption Behavior in some Calcareous Soils using Langmuir, Freundlich, Temkin, and Dubinin-Radushkevich Models" Journal of Soil Sciences and Agricultural Engineering 11(1): 27 – 34.
Kang, CH, Oh, SJ, Shin, Y, Han, SH, Nam, IH and So, JS (2015) "Bioremediation of lead by ureolytic bacteria isolated from soil at abandoned metal mines in South Africa" Ecological Engineering, 402 – 407.
Kapahi, M and Sachdeva, S (2019) "Bioremediation Options for Heavy Metal Pollution" Journal of health & pollution, 9(24), 191203. https://doi.org/10.5696/2156-9614-9.24.191203.
Katsou, E, Malamis, S, Tzanoudaki, M, Haralambous, KJ and Loizidou, M (2011) "Regeneration of natural zeolite polluted by lead and zinc in wastewater treatment systems" J Hazard Mater 189(3); 773 – 786.
Kavak, D (2013) "Removal of lead from aqueous solutions by precipitation: Statistical analysis and modeling" Desalin. Water Treat., 51, 1720–1726.
Kebede, B, Beyene, A, Fufa, F, Megersa, M and Behm, M (2016) "Experimental evaluation of sorptive removal of fluoride from drinking water using iron ore" Appl Water Sci 6, 57 – 65.
Kiran, B, Kaushik, A and Kaushik, CP (2007) "Response surface methodological approach for optimizing removal of Cr (VI) from aqueous solution using immobilized cyanobacterium" Chem. Eng. J. 126, No. 2-3, 147.
Klingberg, T (2010) "Training and plasticity of working memory" Trends Cogn Sci;14:317 - 24.

Kowanga, KD, Gatebe, E, Mauti, GO and Mauti, EM (2016) "Kinetic, sorption isotherms, pseudo-first-order model and pseudo-second-order model studies of Cu(II) and Pb(II) using defatted Moringa oleifera seed powder" The Journal of Phytopharmacology, 5(2), 71 – 78.

Krishnani, KK and Ayyappan, S (2006) "Heavy metals remediation of water using plants and lignocellulosic agrowastes" Rev Environ Contam Toxicol., 188:59-84, DOI: 10.1007/978-0-387-32964-2_2. PMID: 17016916.

Kurniawan, TA, Chan, GY, Lo, WH and Babel, S (2005) "Comparisons of low-cost adsorbents for treating wastewaters laden with heavy metals" Sci Total Environ, 366(2-3):409 - 26. doi: 10.1016/j.scitotenv.2005.10.001.

Langmuir, I (1918) "The adsorption of gases on plane surfaces of glass, mica and platinum" J. Am. Chem. Soc. 40, 1361 – 1403.

Largitte, L and Pasquier, R (2016) "A review of the kinetics adsorption models and their application to the adsorption of lead by an activated carbon" Chemical Engineering Research and Design 109, 495 – 504.

Leung, WC, Wong, MF, Chua, H, Lo, W and Leung, CK (2000) "Removal and recovery of heavy metals by bacteria isolated from activated sludge treating industrial effluents and municipal wastewater" Water Sci. Technol., 41 (12), 233-240.

Liu, Y, Alessi, DS, Owttrim, GW, Kenney, JPL, Zhou, Q, Lalonde, SV, and Konhauser, K (2016) "Cell Surface Acid-Base Properties of the Cyanobacterium Synechococcus: Influences of Nitrogen Source, Growth Phase and N:P Ratios" Acta 187, 179– 194.

Lovei, Magda and Levy, BS (1997) Lead Exposure and Health in Central and Eastern Europe: Evidence from Hungary, Poland and Bulgaria. In Magda Lovei, ed., Phasing Out Lead from Gasoline in Central and Eastern Europe: Health Issues, Feasibility, and Policies, Washington, D.C.: World Bank.

Lovering, TG (1976) Lead in the environment, U.S. Dept. of the Interior, Geological Survey, URL: https://catalog.libraries.psu.edu/catalog/4912481.

Mahmud, HNME, Huq, AO, and binti Yahya, R (2016) "The removal of heavy metal ions from wastewater/aqueous solution using polypyrrole-based adsorbents: a review" Rsc Advances, 6(18), 14778 – 14791.

Martinez, M, Miralles, N, Hidalgo, S, Fiol, N, Villaescusa, I, and Poch, J (2006) "Removal of lead(II) and cadmium (II) from aqueous solutions using grape stalk waste" J. Hazard. Mater. B 133(1 – 3), 203 – 211.

Mason, LH, Harp, JP, and Han, DY (2014) "Pb neurotoxicity: neuropsychological effects of lead toxicity" Biomed Res Int, 840547, Doi: 10.1155/2014/840547.

Mata, YN, Blazquez, ML, Ballester, A, Gonzalez, F, and Munoz, JA (2008) "Characterization of the biosorption of cadmium, lead, and copper with the brown alga Fucus vesiculosus" J Hazard Mater 158(2): 316 – 323.

Matlock, MM, Howerton, BS, and Atwood, DA (2002) "Chemical precipitation of lead from lead battery recycling plant wastewater" Ind. Eng. Chem. Res., 41, 1579–1582.
Mauling, P, Shah, Rodriguez-Couto, S, and Sevinc-Sengor, S (2020) "Emerging Technologies in Environmental Bioremediation" ISBN: 0128198605, 9780128198605.
Masindi, V and Muedi, KL (2018) "Environmental Contamination by Heavy Metals" In Heavy Metals, 115-133). IntechOpen. URL: https://doi.org/10.5772/intechopen.76082.
Meenambal, M, Phugalendy, K, Vasantharaja, C, Prapakaran, S, Vijayan, P (2012) "Phytochemical investigation from FTIR and GC-MS studies of methanol extract of Denolix eltaleaves' International Journal of Chemical and Analytical Science, 3(6), 1446–1448.
Medina-Bellver, JI, Marín, P, Delgado, A, Rodríguez-Sánchez, A, Reyes, E, Ramos, JL, and Marqués, S (2005) "Evidence for in situ crude oil biodegradation after the Prestige oil spill" Environmental microbiology, 7(6), 773 - 779.
Merganpour, AM, Nekuonam, G, Tomaj, OA, Kor, Y, Safari, H, Karimi, K, and Kheirabadi, V (2015) "Efficiency of lead removal from drinking water using cationic resin purolite" Environ. Health Eng. Manag., 2, 41– 45.
Mohammadi, T, Razmi, A, and Sadrzadeh, M (2004) "Effect of operating parameters on Pb2+ separation from wastewater using electrodialysis" Desalination, 167, 379 - 385.
Mouflih, M, Aklil, A, Jahroud, N, Gourai, M, and Sebti, S (2006) "Removal of lead from aqueous solutions by natural phosphate" Hydrometallurgy, 81(3 – 4), 219 – 225.
Mubarak, NM, Sahu, JN, Abdullah, EC, and Jayakumar, NS (2014) "Removal of heavy metals from wastewater using carbon nanotubes" Separation & Purification Reviews, 43(4): 311 – 38.
Muruganantham, MG, Anbalagan, N, and Ramamurthy (2009) "FT-IR and SEM-EDS comparative analysis of medicinal plants, Eclipta alba Hassk and Eclipta prostrata Linn" Romanian J. Biophys., 19(4), 285 – 294.
MuTthanna, J, Mohammed, A, Firas, and Al-Bayati (2009) "Isolation and identification of antibacterial compounds from Thymus kotschyanus aerial parts and Dianthus caryophyllus flower buds" Phytomedicine, 16(6–7), 632 – 637.
Muthukumaran, M, Raghavan, BG, Subramanian, VV, and Sivasubramanian, V (2005) "Bioremediation of industrial effluents using microalgae" India Hydrobiol., 7, 105 -122.
Neveling, O, Ncube, TMC, Ngxongo, ZP, Chirwa, EMN, and Brink, HG (2022) "Microbial Precipitation of Pb(II) with Wild Strains of Paraclostridium bifermentans and Klebsiella pneumoniae Isolated from an Industrially

Obtained Microbial Consortium" International Journal of Molecular Sciences, 23(20):12255. DOI: https://doi.org/10.3390/ijms232012255.
Nimibofa, A, Newton, EA, Cyprain, AY, and Donbebe, W (2018) "Fullerenes: synthesis and applications" J. Mater. Sci., 7: 22 – 33.
Ojedokun, AT and Bello, OS (2016) "Sequestering heavy metals from wastewater using cow dung" Water Resources and Industry, 1(13), 7 – 13.
Osmari, T, Gallon, R, Schwaab, M, Barbosa-Coutinho, E, Severo, J, and Pinto, J (2013) "Statistical Analysis of Linear and Non-Linear Regression for the Estimation of Adsorption Isotherm Parameters" Adsorption Science & Technology, 31, 433-458, 10.1260/0263-6174.31.5.433.
Otero, R (2018) Encyclopedia of Interfacial Chemistry: Surface Science and Electrochemistry, Seven Volume, Institute of Physical and Theoretical Chemistry, University of Bonn, Bonn, Germany.
Pacheco, MM, Hoeltz, M, Moraes, M, and Schneider, RC (2015) "Microalgae: cultivation techniques and wastewater phycoremediation" J Environ Sci Health Part A Toxic/Hazard Subst Environ Eng 50:585 – 601. ISSN:1093-4529 Doi:10.1080/10934529.2015.994951.
Palma, H, Killoran, E, Sheehan, M, Berner, F, and Heimann, K (2017) "Assessment of microalga biofilms for simultaneous remediation and biofuel generation in mine tailings water" Bioresource Technology, 234, 327–335, DOI: 10.1016/j.biortech.2017.03.063.
Panchanadikar, VV, and Das, RP (1994) "Biosorption process for removing lead(II) ions from aqueous effluents using Pseudomonas sp." Intern. ~ Environmental Studies 46, 243 - 250.
Patel, V and Shah, K (2014) "Petroleum hydrocarbon pollution and its biodegradation" International Journal of Chemtech Applications, 2, 63 - 80.
Peer, WA, Baxter, IR, Richards, EL, Freeman, JL, and Murphy, AS (2006) Phytoremediation and hyperaccumulator plants. Molecular biology of metal homeostasis and detoxification: from microbes to man, 299-340. ISSN: 1610-6970, DOI: 10.1007/4735_100.
Peens, J, Wu, WY, and Brink, HG (2018) "Microbial Pb(II) precipitation: The influence of elevated Pb(II) concentrations" Chem. Eng. Trans. 64, 439 – 444.
Perpetuo, E, Barbieri, C, and Nascimento, C (2011) "Engineering Bacteria for Bioremediation" Progress in Molecular and Environmental Bioengineering – From Analysis to Technology Applications, DOI: 10.5772/19546.
Pezoti, O, Cazetta, AL, Bedin, K, Souza, LS, Martins, AC, Silva, TL, Santos-Junior, OO, Vissntainer, JV, and Almeida, VC (2016) "NaOH-activated carbon of high surface area produced from guava seeds as a high-efficiency adsorbent for amoxicillin removal: Kinetic isotherm and thermodynamic studies" Chemical Engineering Journal, 288: 778 – 788.
Polanyi, M (1932) "Section III. – Theories of the adsorption of gases. A general survey and some additional remarks. Introductory paper to section III" Trans. Faraday Soc., 28, 316 – 333.

Qu, X, Zhao, Y, Yu, R, Li, Y, Falzone, C, Smith, G and Ikehata, K (2016) "Health effects associated with wastewater treatment, reuse, and disposal" Water Environment Research, 88(10), 1823-1855.

Raghukumar, C, Vipparty, V, David, J and Chandramohan, D (2001) "Degradation of crude oil by marine cyanobacteria" Appl. Microbiol. Biotechnol., 57, 433 - 436.

Richards, JC and Rodgers, TS (2014) Approaches and Methods in Language Teaching. Cambridge, UK: Cambridge University Press; 2014.

Robalds, A, GM Naja, and M Klavins (2016) "Highlighting inconsistencies regarding metal biosorption" In: Journal of Hazardous Materials 304, pp. 553–556. ISSN: 18733336. DOI: 10.1016/j.jhazmat.2015.10.042.

Rozada, F, Otero, M, Mor´an, A and García, AI, (2008) "Adsorption of heavy metals onto sewage sludge-derived materials" Bioresour. Technol., 99, 6332 – 6338.

Rushikesh, N, Rajdeep, P, Manish, N and Bhaskar, C (2018) "Priority based functional group identification of organic molecules using machine learning" The ACM India Joint International Conference, 201 – 209, DOI:10.1145/3152494.3152522.

Saeed, A, Iqbal, M and Akhtar, MW (2005) "Removal and recovery of lead(II) from single and multiple (Cd, Cu, Ni, Zn) solutions by crop milling waste (black gram husk)" J. Hazard. Mater., 11, 65 – 73.

Salimon, J, Salih, N and Abdullah, B (2011) "Improvement of Physicochemical Characteristics of Monoepoxide Linoleic Acid Ring Opening for Biolubricant Base Oil" Journal of biomedicine & biotechnology., 196565, 10.1155/2011/196565.

Sarabjeet-Singh, A and Dinesh, G (2007) "Microbial and plant derived biomass for removal of heavy metals from wastewater" Bioresource Technology, Volume 98, Issue 12, 2243-2257, ISSN 0960-8524, DOI: https://doi.org/10.1016/j.biortech.2005.12.006.

Saxena, A, Gupta, V and Saxena, S (2020) "BIOREMEDIATION: A GREEN APPROACH TOWARDS THE TREATMENT OF SEWAGE WASTE" J. Phytol. Res 33(2)., 171 – 187, ISSN: 0970-5767.

Schirnding, VY, Mathee, A, Robertson, P, Strauss, N and Kibel, M (2001), "Distribution of blood Lead Levels in Selected Cape Peninsula Suburbs Subsequent to Reductions in Petrol Lead" No.10., 870 - 872.

Schock, MR (1989a) "Understanding lead corrosion control strategies" Journal of the American Water Works Association, 81:88.

Schock, MR (1990b) "Causes of temporal variability of lead in domestic plumbing systems" Environmental monitoring and assessment,15:59.

Seiler, H, Sigel, A and Sigel, H (1994) Handbook on Metals in Clinical and Analytical Chemistry, Vol. 483, 1, 1994, p. 753.

Selatnia, A, Boukazoula, A, Kechid, N, Bakhti, MZ, Chergui, A and Kerchich, Y (2004) "Biosorption of lead (II) from aqueous solution by a bacterial dead Streptomyces rimosus biomass" Biochem. Eng. J., 19, 127-135.

Shams, FA, Kumar, PS, Mahtabin, RR, Anika, TC, Samiha, NN, Rafa, TMI, Mahlia, HC and Ong, MM (2022) "Heavy metal toxicity, sources, and remediation techniques for contaminated water and soil" Environmental Technology & Innovation, Volume 25, 102114, ISSN 2352-1864, https://doi.org/10.1016/j.eti.2021.102114.

Shamuyarira, K and Gumbo, J (2014) "Assessment of Heavy Metals in Municipal Sewage Sludge: A Case Study of Limpopo Province, South Africa" International Journal of Environmental Research and Public Health, 11, 2569 – 2579.

Sharma, GK and Khan, SA (2013) "Bioremediation of Sewage Wastewater Using Selective Algae for Manure Production" International Journal of Environmental Engineering and Management, ISSN 2231-1319, Volume 4, Number 6, 573-580.

Sherlock, JC and Quinn, MJ (1986) "Relationship between blood lead concentrations and dietary lead intake in infants: the Glasgow Duplicate Diet Study 1979-1980" Food additives and contaminants, 3:167 - 176.

Sibanda, T, Selvarajan, R and Tekere, M (2015) "Urban effluent discharges as causes of public and environmental health concerns in South Africa's aquatic milieu" Environ. Sci. Pollut. Res., 22, 18301 – 18317, DOI: 10.1007/s11356-015-5416-4.

Sign and Symptoms of Lead Poisoning. Available from: https://www.reverehealth.com/live-better/signs-symptoms-lead-poisoning/. [Last accessed on 2023 Mar 27].

Singh, CK, Sahu, JN, Mahalik, KK, Mohanty, CR, Mohan, BR and Meikap, BC (2008) "Studies on the removal of Pb(II) from wastewater by activated carbon developed from Tamarind wood activated with sulphuric acid" Journal of Hazardous Materials 153(1 – 2), 221 – 228.

Singh, N and Gupta, SK (2016) "Adsorption of heavy metals: A review" Int. J. Innov. Res. Sci. Eng. Technol., 5(2): 2267 – 81.

Singh, V, Tiwari, A, and Das, M (2016) "Phyco-remediation of industrial wastewater and flue gases with algal-diesel engenderment from micro-algae: A review" Fuel, 173, 90–97, DOI: 10.1016/j.fuel.2016.01.031.

Sinha, SN and Biswas, K (2014) "Bioremediation of lead from river water through lead-resistant purple-nonsulfur bacteria" International Research Publication House, 2(1), 11 – 14.

Statista (2021). Global lead mine production 2010 - 2020. URL: https://www.statista.com/statistics/264871/production-of-lead-worldwide/

Subramanyam, B and Das, A (2014) "Linearised and non-linearised isotherm models optimization analysis by error functions and statistical means" Journal of Environmental Health Science & Engineering, 12 (1): 1 – 6.

Tan, KL and Hameed, BH (2017) "Insight into the adsorption kinetics models for the removal of contaminants from aqueous solutions" J. Taiwan Inst. Chem. Eng. 74, 25–48, https://doi.org/10.1016/j.jtice.2017.01.024.
Tawfik, AS (2022) "Kinetic models and thermodynamics of adsorption processes: classification" Interface Science and Technology, Elsevier, Volume 34, 65 – 97.
Tan, DT, Poh, PE and Chin, SK (2017) "Microorganism preservation by convective air drying – A review" Drying Technology, DOI: 10.1080/07373937.2017.1354876.
Tan, KL, and Hameed, BH (2017) "Insights into the adsorption kinetics models for the removal of contaminants from aqueous solutions" Journal of the Taiwan Institute of Chemical Engineers, 74: 25 – 48.
Tao, Y, Yuan, Z, Xiaona, H and Wei, M (2012) "Distribution and bioaccumulation of heavy metals in aquatic organisms of different trophic levels and potential health risk assessment from Taihu lake, China" Ecotox Environ Safe 81., 55 – 64.
Tao, Y, Zhang, C and Lü, T (2020) "Removal of Pb(II) Ions from Wastewater by Using Polyethyleneimine-Functionalized Fe 3 O 4 Magnetic Nanoparticles" Applied Sciences, 10, 948.
Taty-Costodes, VC, Fauduet, H, Porte, C and Delacroix, A (2003) "Removal of Cd(II) and Pb(II) ions, from aqueous solutions, by adsorption onto sawdust of Pinus sylvestris" J. Hazard. Mater. 105(1 – 3), 121 – 142.
Tong, S, von-Schirnding, YE and Prapamontol, T (2000) "Environmental lead exposure: a public health problem of global dimensions" Bull World Health Organ, 78(9), 1068 – 77. URL: https://www.who.int/bulletin/archives/78(9)1068.pdf
Thapa, B, Kc, AK and Ghimire, A (2012) "A review on bioremediation of petroleum hydrocarbon contaminants in soil" Kathmandu university journal of science, engineering and technology, 8(1), 164 - 170.
The National Institute for Occupational Safety and Health (NIOSH). URL: https://www.cdc.gov/niosh/topics/lead/health.html
Tiwari, S and Tripathi, IP (2012) "Lead Pollution - An Overview" Int. Res. J. Environment Sci., 1(5), 84 - 86.
Tiwari, S, Tripathi, I and Tiwari, HI (2013) "Effects of Lead on Environment" International Journal of Emerging Research in Management & Technology, ISSN: 2278 – 9359.
Torres, E (2020) "Biosorption: A Review of the Latest Advances" Processes, 8(12), 1584. URL: https://doi.org/10.3390/pr8121584.
Toxicological Profile for Lead. URL: https://www.atsdr.cdc.gov/toxprofiles/tp13-c4.pdf
Tran, HN, You, SJ, Hosseini-Bandegharaei, A and Chao, HP (2017) "Mistakes and inconsistencies regarding adsorption of contaminants from aqueous

solutions: A critical review" Water Research 120, 88–116. ISSN: 18792448. DOI: 10.1016/j.watres.2017.04.014.
Tripathi, A and Ranjan, MR (2015) "Heavy metal removal from wastewater using low-cost adsorbents" JBioremedBiodeg., 6(6): 315.
Tripathi, M, Singh, DN, Prasad, N and Gaur, R (2021) "Advanced Bioremediation Strategies for Mitigation of Chromium and Organics Pollution in Tannery" Rhizobiont in Bioremediation of Hazardous Waste, Springer, Singapore., 195 – 215.
U.S. Department of Health and Human Services (2007) Toxicological profile for Lead (update) [http://www.atsdr.cdc.gov/toxprofiles/tp13.pdfpdf (PDF 4901KB, 582 pages)] Public Health Service Agency for Toxic Substances and Disease Registry.
U.S. Geological Survey. Mineral Commodity Summaries (2019) URL: https://pubs.usgs.gov/periodicals/mcs2020/mcs2020.pdf.
USEPA (2003) Non-halogenated organics using GC/FID, USEPA, Washington, DC.
Van-Hille, RP, Antunes, A, Sanyahumbi, D, Nightingale, L, and Duncan, JR (2003) Development of integrated biosorption systems for the removal and/or recovery of heavy metals from mining and other industrial wastewaters, and determination of the toxicity of metals to bioremediation processes: WRC Report No. 1243/1/03. Tech. rep. Water Research Commission.
Van-Veenhuyzen, B, Brink, H, and Chirwa, E (2021a) “Microbial Pb(ii) Precipitation: the Role of Biosorption as a Pb(ii) Removal Mechanism” Chemical Engineering Transactions. 86. 181-185. 10.3303/CET2186031.
Van-Veenhuyzen, B, Ho ̈rstmann, C, Peens, J, and Brink, HG (2020) “Bioremediation and biorecovery of aqueous lead by local lead-resistant organisms” Emerging Technologies in Environmental Bioremediation, Elsevier, 407 – 424.
Van-Veenhuyzen, B, Tichapondwa, S, Cilliers, C, Chirwa, E, and Brink, H (2021b) “High Capacity Pb(II) Adsorption Characteristics onto Raw- and Chemically Activated Waste Activated Sludge” Journal of Hazardous Materials, 416. 125943. 10.1016/j.jhazmat.2021.125943.
Veglio, F, and Beolchini, F (1997) “Removal of metals by biosorption: a review” Hydrometallurgy, 44(3): 301 – 16.
Vishan, I, Saha, B, Sivaprakasam, S, and Kalamdhad, A (2019) “Evaluation of Cd(II) biosorption in aqueous solution by using lyophilized biomass of novel bacterial strain Bacillus badius AK: biosorption kinetics, thermodynamics and mechanism” Environ Technol Innov 14: 100323.
Volesky, B (1994a) “Advances in biosorption of metals: Selection of biomass types” FEMS Microbiology Reviews, Volume 14, Issue 4, 291-302, ISSN 0168-6445, URL: https://www.sciencedirect.com/science/article/pii/0168644594900469.

Volesky, B and Holan, ZR (1995b) “Biosorption of heavy metals” Biotechnol. Prog. 11, 235-250.
Vunain, E, Mishra, AK, and Mamba, BB (2016) “Dendrimers, mesoporous silicas and chitosan-based nanosorbents for the removal of heavy-metal ions: a review” International journal of biological macromolecules”, 86: 570 – 86.
Wang, J and Guo, X (2020) “Adsorption kinetic models: physical meanings, applications, and solving methods. J. Hazard. Mater. 390, 122156.
Wang, J and Guo, X (2020) “Adsorption isotherm models: classification, physical meaning, application and solving method” Chemosphere 258, 127279.
Wang, X., Liang, X., Wang, Y., Wang, X., Liu, M., Yin, D., Xia, S., Zhao, J., Zhang, Y., 2011. Adsorption of Copper (II) onto activated carbons from sewage sludge by microwave-induced phosphoric acid and zinc chloride activation. Desalination 278, 231–237. https://doi.org/10.1016/j.desal.2011.05.033.
Wear, LS, Acuña, W, McDonald, R, and Font, C (2021) “Sewage pollution, declining ecosystem health, and cross-sector collaboration” Biological Conservation, 255(5), 109010, ISBN: 0006-3207, URL: https://doi.org/10.1016/j.biocon.2021.109010.
Webber, TW and Chakkravorti, RK (1974) “Pore and solid diffusion models for fixed-bed adsorbers” AIChE J, 20, 228 – 238.
Weber, WJ and Morris, JC (1963) “Kinetics of adsorption on carbon from solution” J Sanit Eng Div 89, 31–60.
Welp, G and Bru ̈mmer, GW (1999) “Adsorption and solubility of ten metals in soil samples of different composition” Journal of plant nutrition and soil science, 16(2), 155 – 161.
WHO (2006a) “Guidelines for the Safe Use of Wastewater, Excreta and Greywater, vol. 3” World Health Organisation Press, Geneva, Switzerland.
WHO (1997b) “Nitrogen oxides” Environmental Health Criteria 2nd edn No. 54., Geneva, Switzerland.
Wong, PK, Lam, KC, and So, CM (1993) “Removal and recovery of Cu(II) from Industrial effluent by immobilized cells of Pseudomonas putida II-11” Appl. Microbiol. Biotechnol. 1993, 39, 127 – 131.
Wu, Q, Leung, JY, Geng, X, Chen, S, Huang, X, Li H, et al., (2015) “Heavy metal contamination of soil and water in the vicinity of an abandoned e-waste recycling site: Implications for dissemination of heavy metals” Sci Total Environ, 506-507: 217-25.
Wuang, SC, Luo, YD, Wang, S, Chua, PQD, and Tee, PS (2016) “Performance assessment of biofuel production in an algae-based remediation system” Journal of Biotechnology, 221, 43 – 48. doi:10.1016/j.jbiotec.2016.01.024.
Yang, RT (1997) Gas separation by adsorption processes, Imperial College Press, London, U.K.

Yao, J, Chen, Y, Yu, HQ, and Liu, T (2016) “Efficient and fast removal of Pb(II) by facile prepared magnetic vermiculite from aqueous solution” Rsc. Adv.; 103: 101353 – 101360.

Yarkandi, NH (2014) “Removal of lead (II) from wastewater by adsorption” International Journal of Current Microbiology and Applied Sciences 3(4), 207 – 228.

Zeng, L, Li, X, and Liu, J (2004) “Adsorptive removal of phosphate from aqueous solutions using iron oxide tailings” Water Res 38, 1318–1326.

Zhao, D, Yu, Y, and Chen, JP (2016) “Treatment of lead contaminated water by a PVDF membrane that is modified by zirconium, phosphate and PVA” Water Res., 101, 564–573.

Zhang, QH, Yang, WN, Ngo, HH, Guo, WS, Jin, PK, Dzakpasu, M, Yang, SJ, Wang, Q, Wang, XC, and Ao, D (2016) “Current status of urban wastewater treatment plants in China” Environment international, 92, 11 - 22.

Zhou, F, Wang, H, Fang, S, Zhang, W, and Qiu, R (2015) “Pb(II), Cr(VI) and atrazine sorption behavior on sludge-derived biochar: role of humic acids” Environ. Sci. Pollut. Res., 22, 16031 – 16039.

Zimmo, OR, Al-Sa’ed, RM, Van der Steen, NP, and Gijzen, HJ (2002) “Process performance assessment of algae-based and duckweed-based wastewater treatment systems” Water. Sci. Technol. 45, 91-101.

Appendix A Kinetic fits

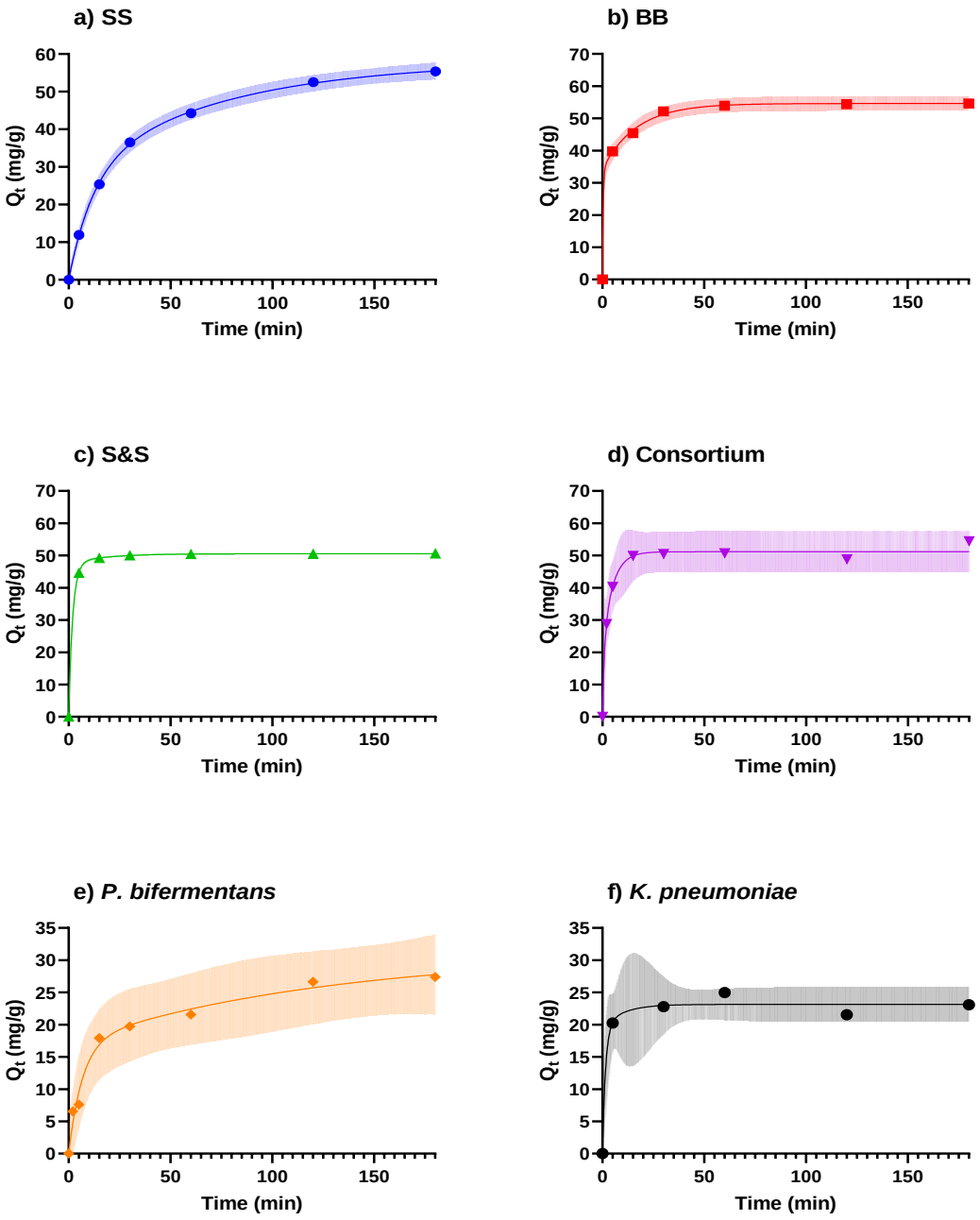

Figure 7: Two-phase pseudo-first-order kinetics of Pb(II) onto metabolically inactive (a) sewage sludge, (b) bran-based filler bacteria, (c) salt-and-starch based filler bacteria, (d) consortium, (e) P. bifermentans, and (f) K. pneumoniae.

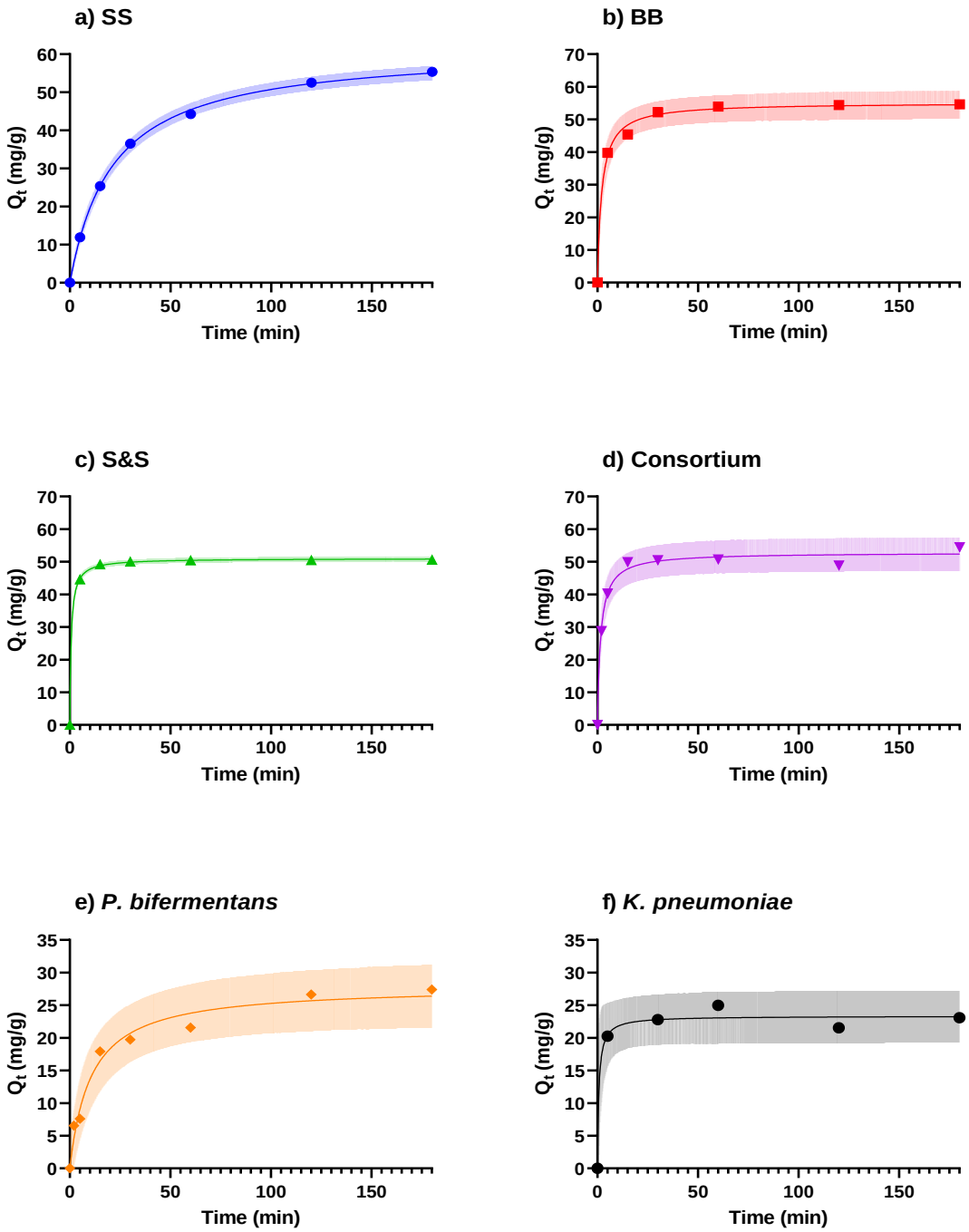

Figure 8: Pseudo-second-order kinetics of Pb(II) onto metabolically inactive (a) sewage sludge, (b) bran-based filler bacteria, (c) salt-and-starch based filler bacteria, (d) consortium, (e) P. bifermentans, and (f) K. pneumoniae.

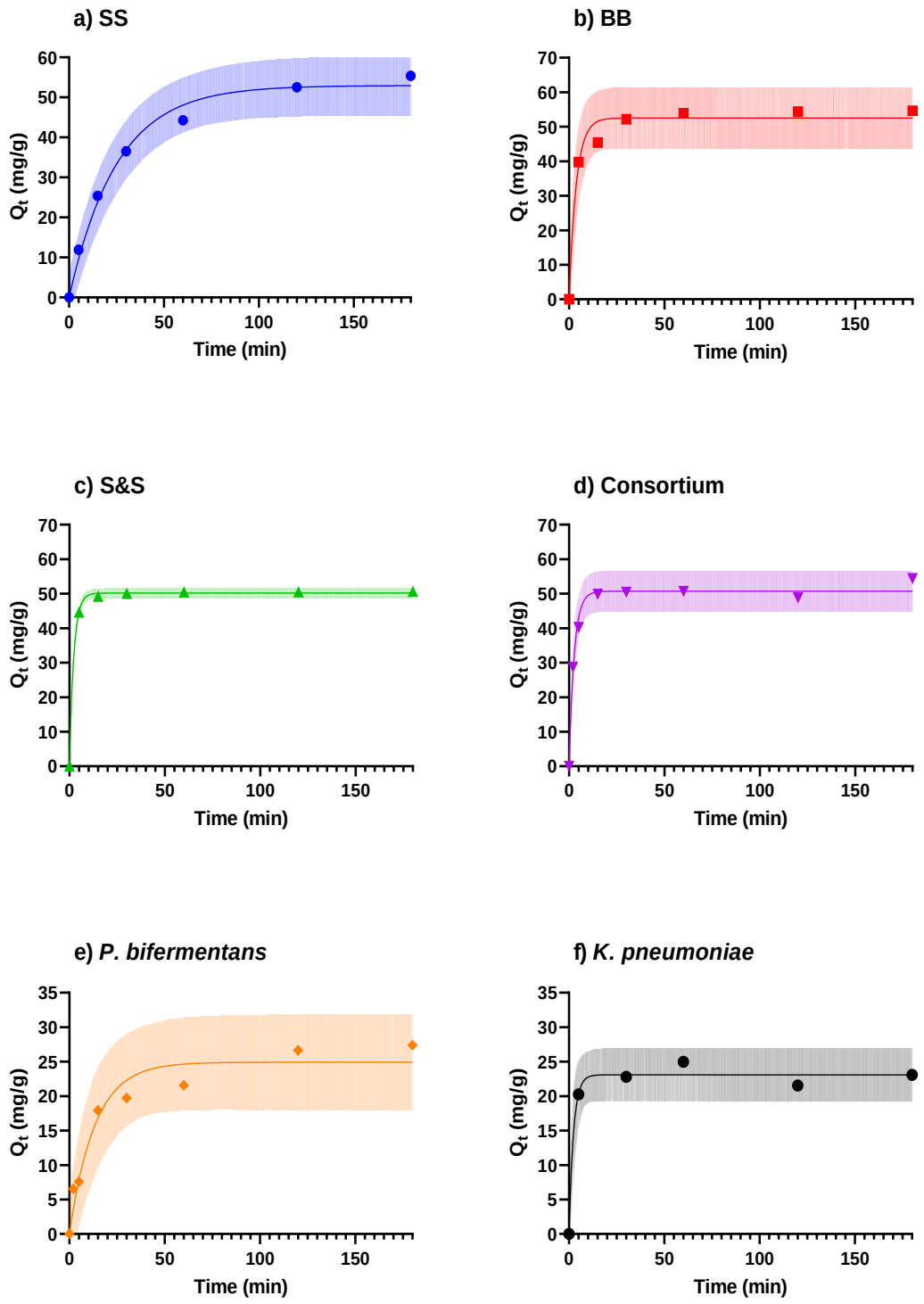

Figure 9: Pseudo-first-order kinetics of Pb(II) onto metabolically inactive (a) sewage sludge, (b) bran-based filler bacteria, (c) salt-and-starch based filler bacteria, (d) consortium, (e) P. bifermentans, and (f) K. pneumoniae.

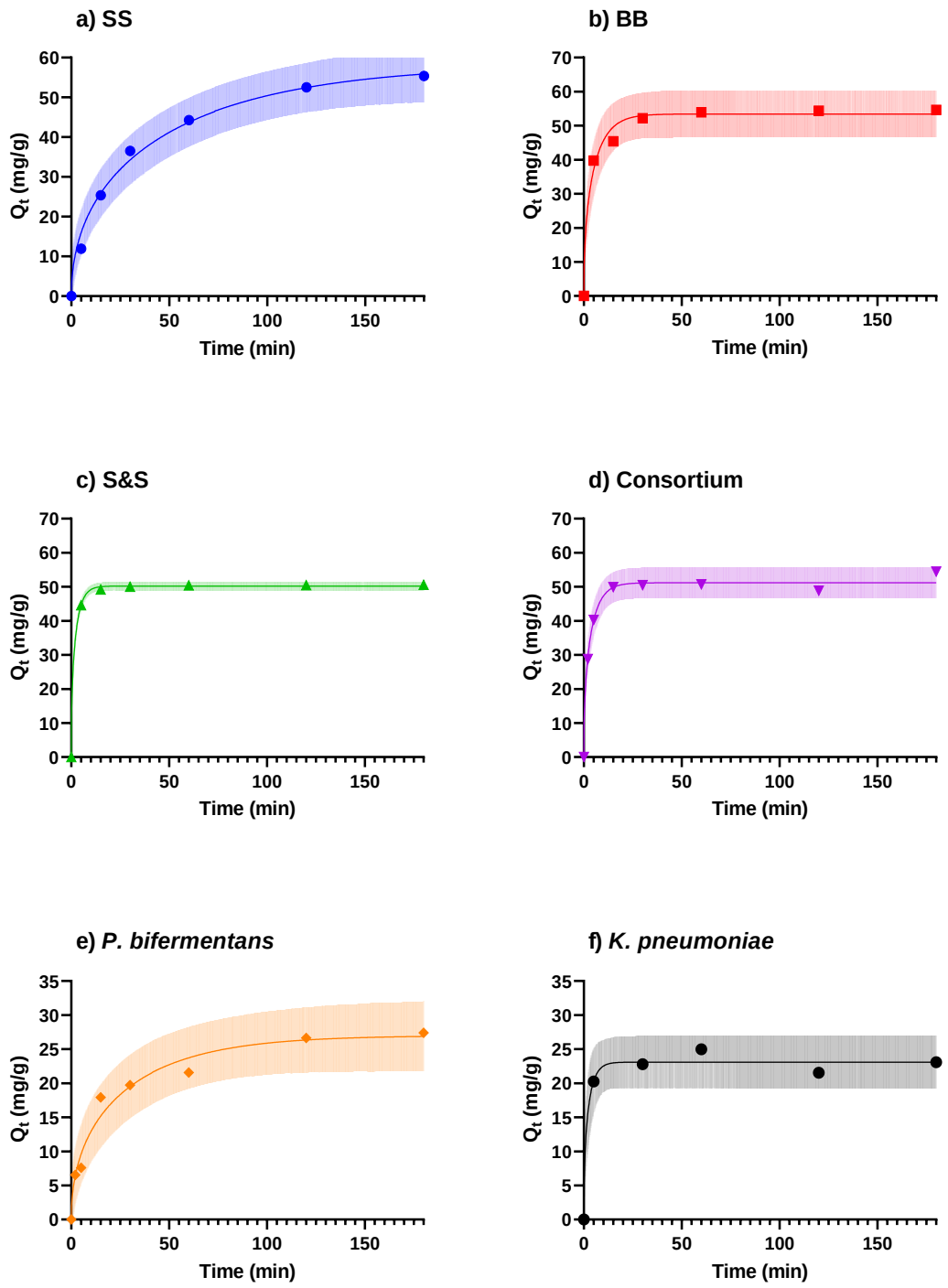

Figure 10: Cranks mass transfer model of Pb(II) onto metabolically inactive (a) sewage sludge, (b) bran-based filler bacteria, (c) salt-and-starch based filler bacteria, (d) consortium, (e) P. bifermentans, and (f) K. pneumoniae.

Appendix B Isotherm fits

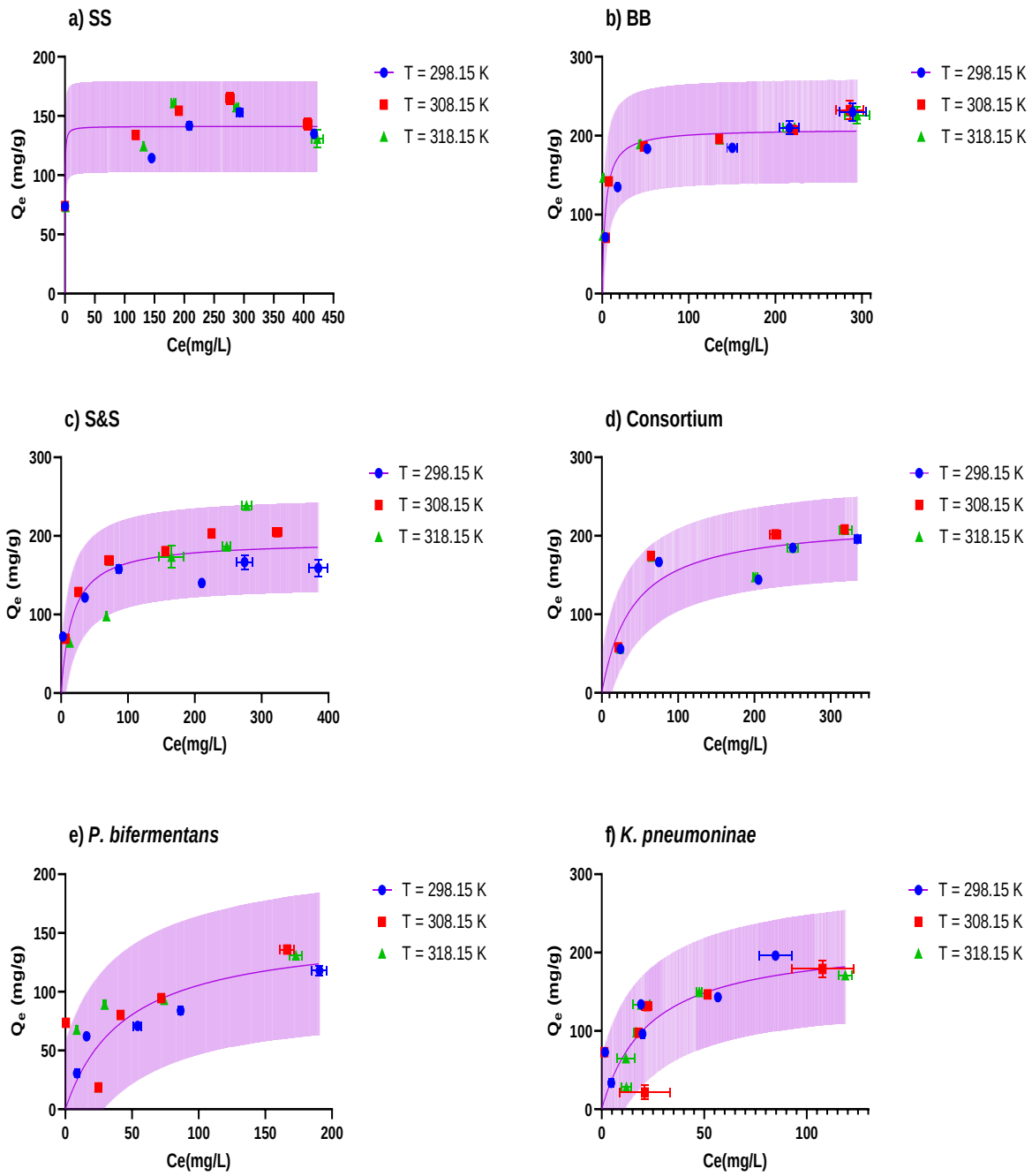

Figure 11: Langmuir isotherm for metabolically inactive (a) sewage sludge, (b) bran-based filler bacteria, (c) salt-and-starch filler bacteria, (d) consortium, (e) P. bifermentans, and (f) K. pneumoniae with a 95% prediction interval in the shaded area.

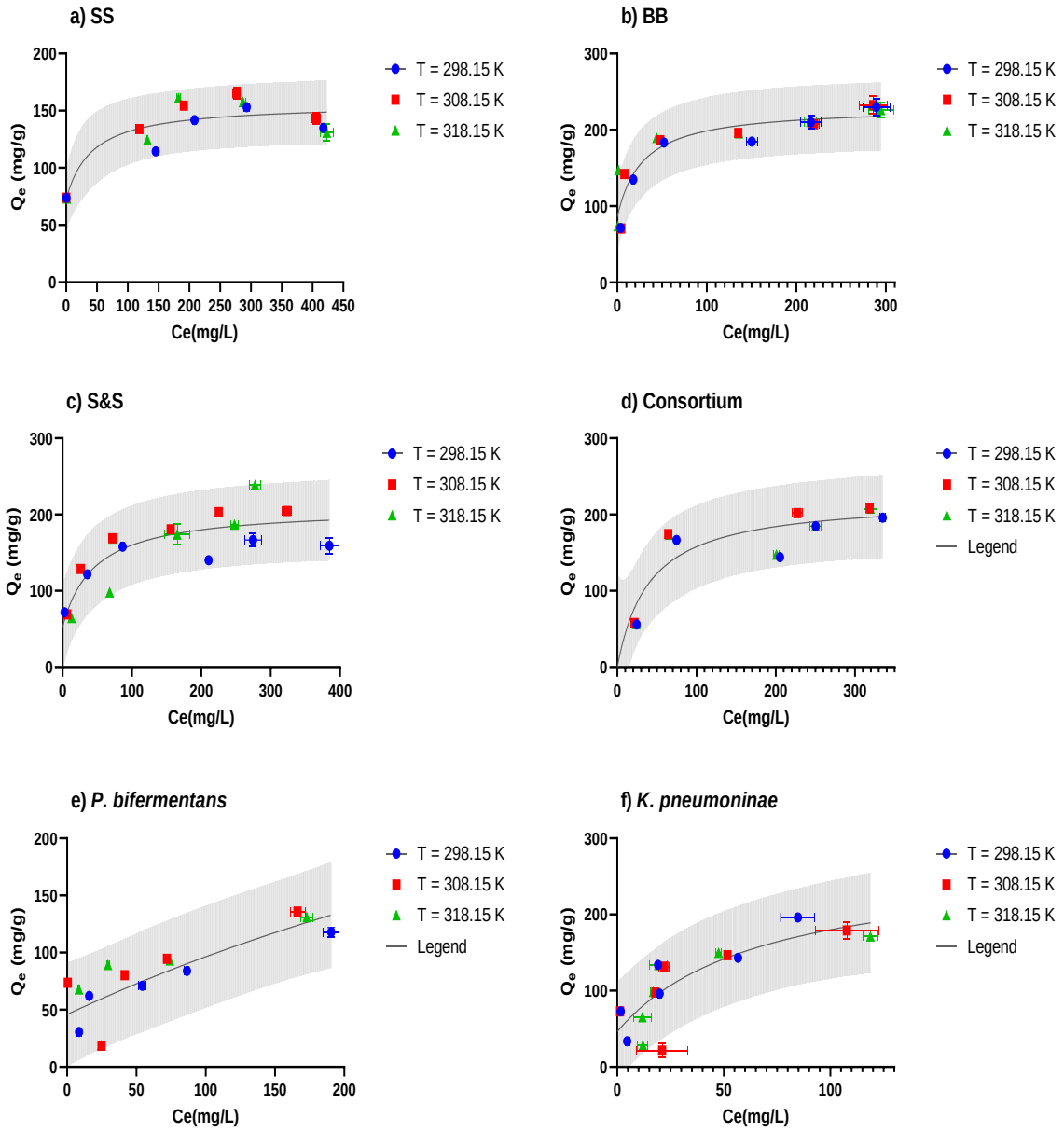

Figure 12: Two – surface Langmuir isotherm for metabolically inactive (a) sewage sludge, (b) bran-based filler bacteria, (c) salt-and-starch based filler bacteria, (d) consortium, (e) P. bifermentans, and (f) K. pneumoniae with a 95% prediction interval in the shaded area.

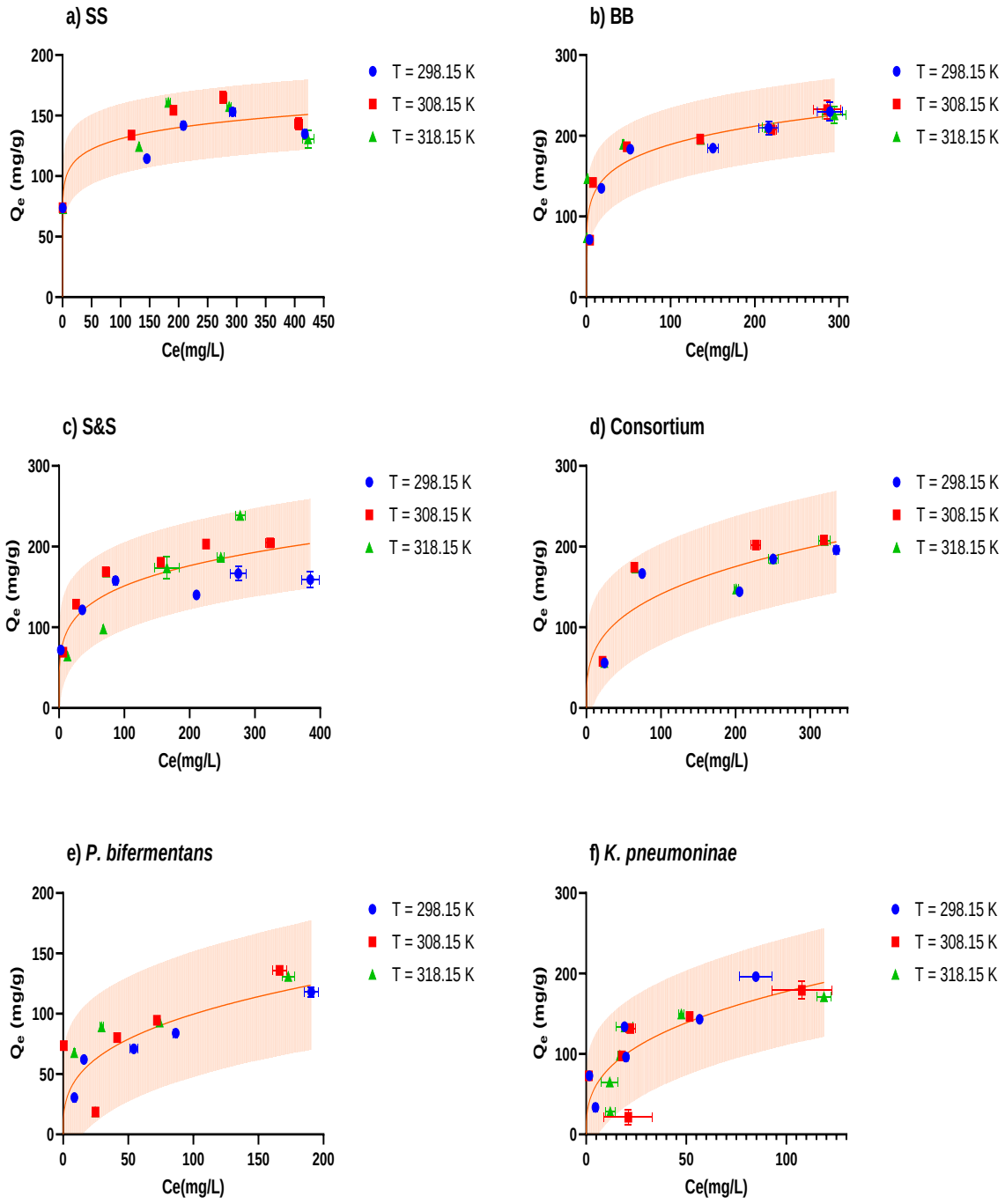

Figure 13: Freundlich isotherm for metabolically inactive (a) sewage sludge, (b) bran – based filler bacteria, (c) salt – and – starch-based filler bacteria, (d) consortium, (e) P. bifermentans, and (f) K. pneumoniae with a 95% prediction interval in the shaded area.

Appendix C FTIR spectra results

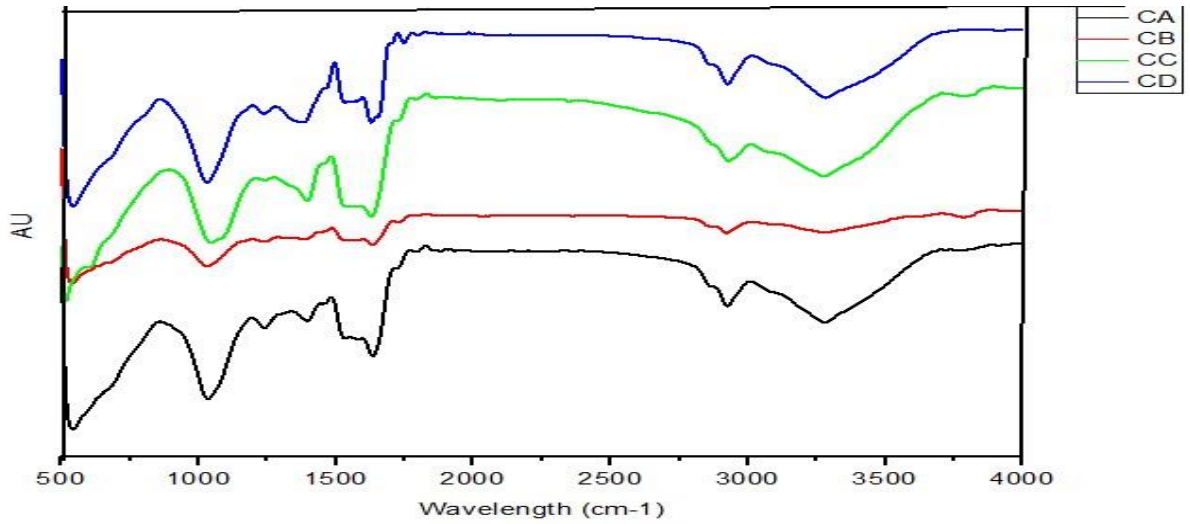

Figure 14: FTIR spectra for sewage sludge CA) after a growth period of 24 h, CB) after oven drying for 24 h at 74°C, CC) after exposure to $Pb(NO_3)_2$, and CD)14 h after adding $Pb(NO_3)_2$.

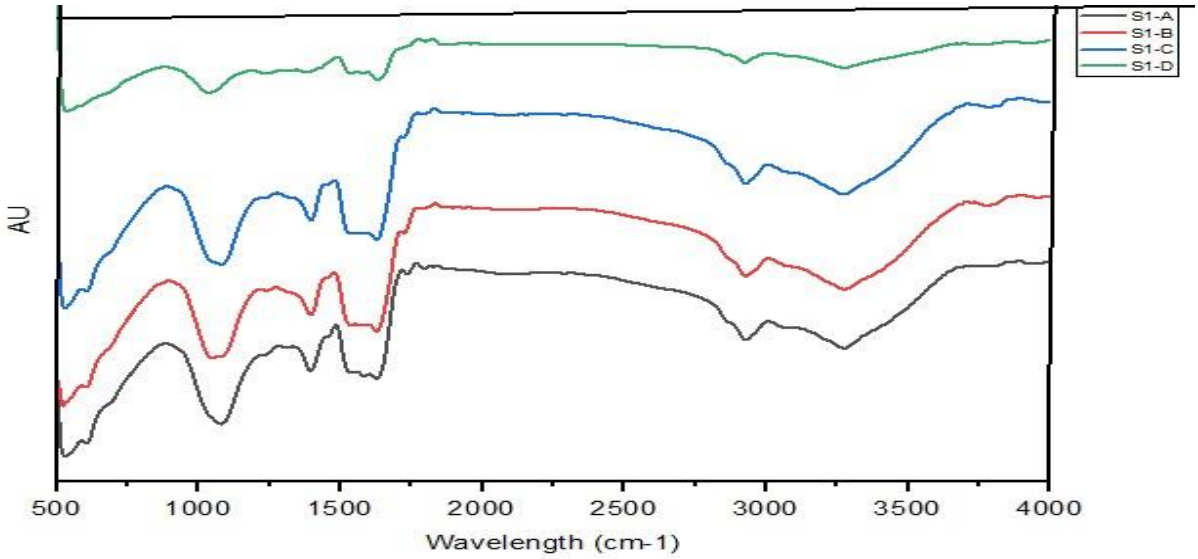

Figure 15: FTIR spectra for bran-based filler bacteria S1-A) after a growth period of 24 h, S1-B) after oven drying for 24 h at 74°C, S1-C) after exposure to $Pb(NO_3)_2$, and S1-D)14 h after adding $Pb(NO_3)_2$.

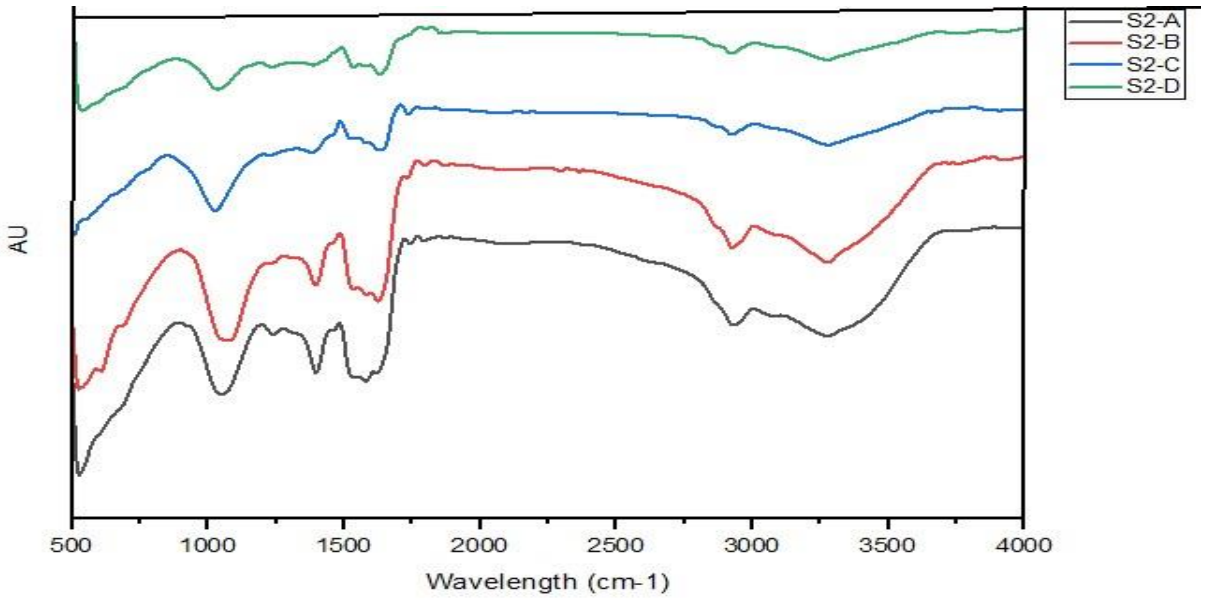

Figure 16: FTIR spectra for salt-and-starch filler based bacteria S2-A) after a growth period of 24 h, S2-B) after oven drying for 24 h at 74°C, S2-C) after exposure to $Pb(NO_3)_2$ *and S2-D)14 h after adding* $Pb(NO_3)_2$.

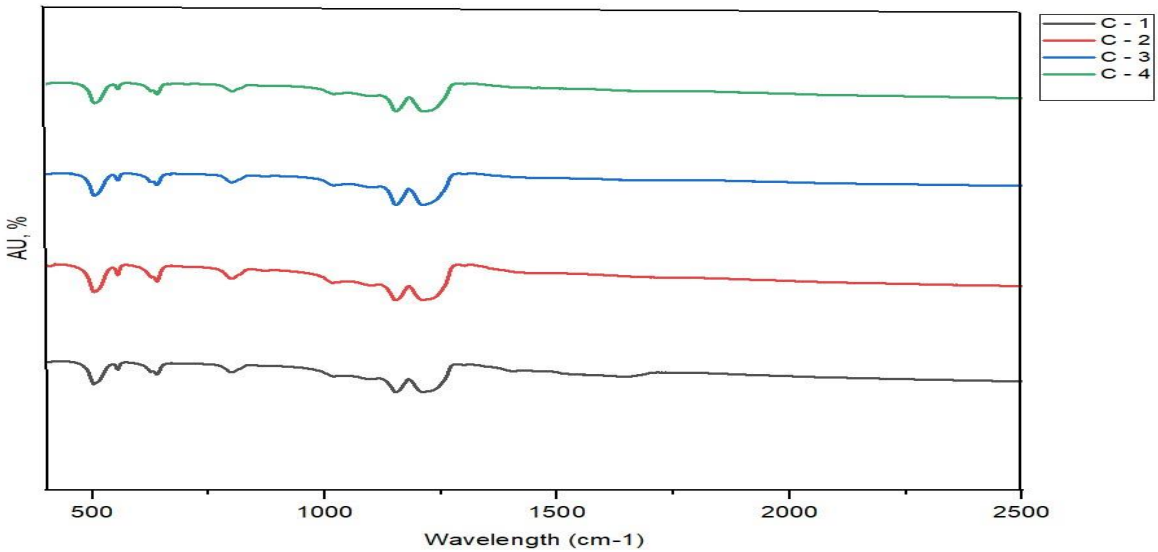

Figure 17: FTIR spectra of the consortium C-1) after a growth period of 24 h, C-2) after oven drying at 74C for 24 h, C-3) after exposure to 100 ppm of $Pb(NO_3)_2$, *and C-4) 14 h after adding 100 ppm of* $Pb(NO_3)_2$.

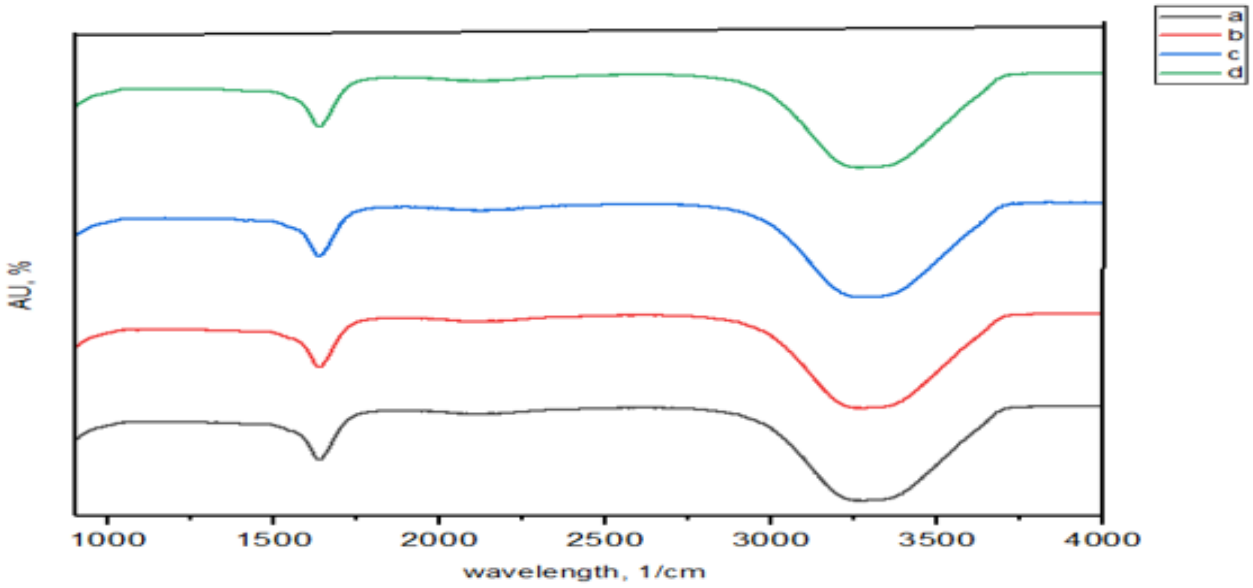

Figure 18: FTIR spectra of K. pneumoniae a) after a growth period of 24 h, b) after oven drying for 24 h at 74°C, c) after exposure to $Pb(NO_3)_2$, and d)14 h after adding $Pb(NO_3)_2$.

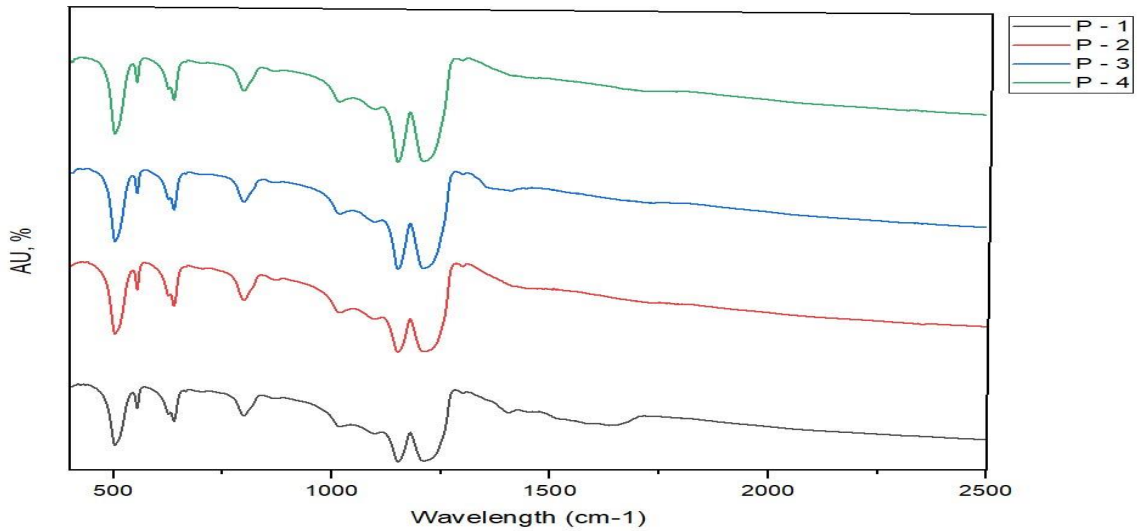

Figure 19: FTIR spectra of P. bifermentans P-1) after a growth period of 24 h, P-2) after oven drying at 74°C for 24 h, P-3) after exposure to 100 ppm of $Pb(NO_3)_2$, and P-4) 14 h after adding 100 ppm of $Pb(NO_3)_2$.

Appendix D SEM – EDS results

This appendix contains the results of the Energy – Dispersive X-ray Spectroscopy (EDS) Analysis for the metabolically inhibited SS, BB, S&S, Cons, PB, and KP.

Table 21: EDS results for Sewage Sludge (SS)

Element	Line Type	Apparent Concentration	k Ratio	Wt%	Wt% Sigma
C	K series	115.35	1.15351	63.79	0.37
N	K series	9.60	0.01709	6.15	0.51
O	K series	42.78	0.14395	26.63	0.18
Na	K series	6.23	0.02630	1.37	0.02
Mg	K series	0.53	0.00350	0.13	0.01
Al	K series	0.11	0.00080	0.02	0.00
Si	K series	0.59	0.00465	0.11	0.00
P	K series	2.96	0.01658	0.37	0.01
S	K series	3.36	0.02896	0.66	0.01
Cl	K series	1.11	0.00972	0.22	0.01
K	K series	1.42	0.01202	0.26	0.01
Ca	K series	0.84	0.00754	0.16	0.01
Fe	K series	0.25	0.00245	0.05	0.01
Pb	M series	0.37	0.00347	0.08	0.03
Total:				100.00	

Table 22: EDS results for Bran-Based Filler Bacteria (BB)

Element	Line Type	Apparent Concentration	k Ratio	Wt%	Wt% Sigma
C	K series	43.36	0.43363	59.62	0.64
N	K series	7.52	0.01339	8.29	0.87
O	K series	16.23	0.05461	18.84	0.31
Na	K series	3.13	0.01322	1.19	0.03
Mg	K series	0.53	0.00353	0.22	0.02
Al	K series	2.17	0.01558	0.79	0.02
Si	K series	4.61	0.03651	1.56	0.03
P	K series	7.37	0.04120	1.66	0.03
S	K series	2.68	0.02313	0.96	0.03
Cl	K series	0.36	0.00317	0.14	0.01
K	K series	1.12	0.00952	0.38	0.02
Ca	K series	2.36	0.02111	0.80	0.02
Ti	K series	0.28	0.00283	0.11	0.02
Fe	K series	1.08	0.01076	0.43	0.03
W	L series	0.00	0.00000	0.00	0.00
Pb	M series	12.78	0.11892	5.03	0.12
Total:				100.00	

Table 23: EDS results for Salt-and-Starch Based Filler Bacteria (S&S)

Element	Line Type	Apparent Concentration	k Ratio	Wt%	Wt% Sigma
C	K series	29.36	0.29360	56.65	0.72
N	K series	4.44	0.00790	6.11	1.01
O	K series	11.76	0.03957	17.27	0.31
Na	K series	0.74	0.00312	0.40	0.03
Al	K series	1.07	0.00772	0.55	0.02
Si	K series	3.30	0.02616	1.53	0.03
P	K series	4.04	0.02262	1.23	0.04
S	K series	1.04	0.00893	0.51	0.05
Cl	K series	0.30	0.00261	0.17	0.03
K	K series	0.48	0.00410	0.24	0.02
Ca	K series	0.17	0.00154	0.08	0.02
Fe	K series	0.89	0.00889	0.48	0.05
Pb	M series	27.22	0.25331	14.78	0.26
Total:				100.00	

Table 24: EDS results for Consortium (Cons)

Element	Line Type	Apparent Concentration	k Ratio	Wt%	Wt% Sigma
C	K series	37.64	0.37639	53.89	0.37
N	K series	8.43	0.01500	8.83	0.54
O	K series	15.80	0.05316	18.93	0.20
Na	K series	0.51	0.00216	0.23	0.02
P	K series	5.94	0.03321	1.45	0.03
S	K series	0.42	0.00361	0.17	0.04
Cl	K series	0.50	0.00437	0.23	0.02
Pb	M series	36.97	0.34407	16.28	0.16
Total:				100.00	

Table 25: EDS results for Klebsiella pneumoniae (KP)

Element	Line Type	Apparent Concentration	k Ratio	Wt%	Wt% Sigma
C	K series	52.65	0.52652	54.89	0.33
N	K series	15.36	0.02734	13.21	0.46
O	K series	18.12	0.06098	18.72	0.16
Na	K series	2.88	0.01217	1.00	0.02
Mg	K series	0.25	0.00164	0.09	0.01
P	K series	6.34	0.03547	1.23	0.02
S	K series	1.20	0.01033	0.37	0.02
Cl	K series	0.61	0.00536	0.21	0.01
K	K series	0.61	0.00520	0.19	0.01
Ca	K series	1.73	0.01546	0.53	0.01
Mn	K series	0.19	0.00188	0.07	0.01
Fe	K series	0.41	0.00409	0.14	0.01
Pb	M series	27.11	0.25224	9.35	0.09
Total:				100.00	

Table 26: EDS results for Paraclostridium bifermentans (PB)

Element	Line Type	Apparent Concentration	k Ratio	Wt%	Wt% Sigma
C	K series	79.86	0.79865	64.12	0.55
N	K series	13.37	0.02381	12.23	0.71
O	K series	17.19	0.05786	17.53	0.22
Na	K series	0.72	0.00305	0.22	0.02
Mg	K series	0.27	0.00179	0.09	0.01
Al	K series	0.12	0.00087	0.03	0.01
Si	K series	0.21	0.00165	0.06	0.01
P	K series	6.39	0.03576	1.12	0.02
S	K series	2.96	0.02547	0.82	0.02
K	K series	0.25	0.00213	0.07	0.01
Ca	K series	2.76	0.02469	0.73	0.02
Mn	K series	0.26	0.00263	0.08	0.02
Fe	K series	0.17	0.00174	0.05	0.02
Pb	M series	9.31	0.08667	2.85	0.08
Total:				100.00	